Electrically Small Archimedean Spiral Method of Moments Analysis

by
Michael M. Neel
G & C Systems Division

DTIC
ELECTE
MAR 03 1995
S G D

FEBRUARY 1994

NAVAL AIR WARFARE CENTER WEAPONS DIVISION
CHINA LAKE, CA 93555-6001

Approved for public release; distribution is unlimited.

19950227 090

Naval Air Warfare Center Weapons Division

FOREWORD

This report presents the electromagnetic analysis of an electrically small Archimedean spiral. This work was performed at the Naval Air Warfare Center Weapons Division, China Lake, Calif., during fiscal year 1994 in support of an Accelerated Technology Initiative investigating High Temperature Superconducting Antennas sponsored by the Office of Naval Research, Information, Electronics and Surveillance Science and Technology Department (ONR31). This work was monitored initially by Dr. Y. S. Park and subsequently by Dr. Donald H. Liebenberg under fund document N0001494WX35177.

This report is a working document subject to change and was reviewed for technical accuracy by Donald R. Bowling.

Approved by
K. L. Higgins, *Head*
G & C Systems Division
February 1995

Under authority of
D. B. McKinney
RAdm., U.S. Navy
Commander

Released for publication by
S. HAALAND
Head, NAWCWPNS Engineering Group

NAWCWPNS Technical Publication 8245

Published by . . . . . Scientific and Technical Documentation
Collation . . . . . Cover, 23 leaves
First printing . . . . . 26 copies

REPORT DOCUMENTATION PAGE

Form Approved
OMB No. 0704-0188

Public reporting burden for this collection of information is estimated to average 1 hour per response, including the time for reviewing instructions, searching existing data sources, gathering and maintaining the data needed, and completing and reviewing the collection of information. Send comments regarding this burden estimate or any other aspect of this collection of information, including suggestions for reducing this burden, to Washington Headquarters Services, Directorate for Information Operations and Reports, 1215 Jefferson Davis Highway, Suite 1204, Arlington, VA 22202-4302, and to the Office of Management and Budget, Paperwork Reduction Project (0704-0188), Washington, DC 20503.

1. AGENCY USE ONLY *(Leave blank)*	2. REPORT DATE	3. REPORT TYPE AND DATES COVERED
	February 1995	Interim - October 1993-September 1994

4. TITLE AND SUBTITLE
ELECTRICALLY SMALL ARCHIMEDEAN SPIRAL METHOD OF MOMENT ANALYSIS

5. FUNDING NUMBERS
N00014-94-WX-35177

6. AUTHOR(S)
Michael M. Neel

7. PERFORMING ORGANIZATION NAME(S) AND ADDRESS(ES)
Naval Air Warfare Center Weapons Division
China Lake, CA 93555-6001

8. PERFORMING ORGANIZATION REPORT NUMBER
NAWCWPNS TP 8245

9. SPONSORING/MONITORING AGENCY NAME(S) AND ADDRESS(ES)
Dr. Yoon Soo Park
ONR 44GI
Office of Naval Research
Washington, DC

10. SPONSORING/MONITORING AGENCY REPORT NUMBER

11. SUPPLEMENTARY NOTES

12A. DISTRIBUTION/AVAILABILITY STATEMENT
A Statement; Distribution Unlimited

12B. DISTRIBUTION CODE

13. ABSTRACT *(Maximum 200 words)*

(U) This paper presents an analysis of an electrically small archimedean spiral. Method of moment calculations were performed to find the spiral arm current distribution, and optimum arm road impedance over a three-to-one bandwidth.

DTIC QUALITY INSPECTED 4

14. SUBJECT TERMS
Antennas, Method of Moments, Spiral, Impedance

15. NUMBER OF PAGES
45

16. PRICE CODE

17. SECURITY CLASSIFICATION OF REPORT	18. SECURITY CLASSIFICATION OF THIS PAGE	19. SECURITY CLASSIFICATION OF ABSTRACT	20. LIMITATION OF ABSTRACT
UNCLASSIFIED	UNCLASSIFIED	UNCLASSIFIED	UL

Accesion For
NTIS CRA&I ☒
DTIC TAB ☐
Unannounced ☐
Justification .....
By .....
Distribution /
Availability Codes
Dist | Avail and / or Special
A-1

CONTENTS

CONTENTS (Contd.)

Table:

INTRODUCTION

At the beginning of fiscal year 1994, a program was initiated to investigate the application of high-temperature superconducting (HTS) metals to improve the performance of electrically small spirals. By using the very low resistance of these metals, it might be possible to extend the lower frequency of operation by a factor of two to three. This would make it possible to receive frequencies that require the use of much larger airframes than in the past. A program funded by the Army has shown success in the use of a 1-inch-diameter HTS spiral antenna for simple crystal video detected signals, with indication of highly improved sensitivity at lower frequencies. The application of the Navy program this year is centered around the use of a three-inch-diameter HTS spiral to obtain circular polarized radiation/reception and good pattern quality down to at least 500 MHz, and improve the antenna's gain by factors of 10 to 20.

This program is being pursued through two parallel paths. One design approach is being addressed by American Electronic Labs (AEL), with funding through the Office of Naval Research, to build a three-inch-diameter, balun/center fed spiral and test for pattern quality and polarization. The other approach, being pursued here at the Naval Air Warfare Center Weapons Division, China Lake, Calif., is a three-inch-diameter, integrated balun/spiral arm fed spiral. Each design has its possible advantages and shortcomings, which we hope to determine this year.

The primary characteristics of spiral antennas that have encouraged their use are the broadband impedance, gain, and pattern shape, and circular polarization. (A good treatment of this subject is found in Reference 1.) Other antenna designs provide for broadband, linear polarized patterns, but the primary use of the spiral antenna is in areas where circular polarization is required. Driving a spiral antenna down in frequency where its aperture does not allow proper summation of the arm currents will rapidly degrade its polarization quality and the input impedance. In theory, the bandwidth of these quantities depend on the antenna radiating most of its power into free space, which is primarily determined by whether the currents on the arms can get into the correct phase or spatial position relationship. If enough physical space is occupied by the antenna, these conditions will be satisfied. It has not been understood how reducing the spiral arm's electrical resistance will have any effect on the phase of the currents and allow lower frequency use. However, prior practical application indicates that this approach works.

These questions prompted an attempt to analyze and understand better the mechanisms governing spiral antenna radiation, and study the effects incurred when the frequency of operation goes below conventional limits.

Typical analysis of spiral antennas in the past has centered around derivation of closed-form expressions describing the popular "radiation ring" of the antenna. This region is basically described as an "N" wavelength circumference area where adjacent spiral arm currents are in phase, and the total phase shift of these currents is "N" times 2*PI radians. The number N is an integer, 1 or higher. (Refer to Reference 1 for more detailed

discussion.) In recent years, analysis of spiral antennas has been done using programs based on the Method of Moments (MOM) electromagnetic analysis technique. These codes use the antenna wire geometry as the basic starting point, from which the antenna's "Z" or "Y" matrix is calculated. By defining the drive point locations and voltages or currents, the resultant wire currents and radiated field can be obtained. Thus, a detailed picture of the antenna's currents and impedance can be revealed. With careful application, this type of analysis can potentially yield information about the antenna unobtainable any other way.

Analysis of spiral antennas with MOM techniques has been the subject of various articles and at least one book (Reference 2). A number of insights about the mechanisms of the antenna have resulted from these. Prior to 1994, all these analyses have centered around the typical case of a spiral with sufficient diameter to radiate easily. Most have centered around determining optimum arm termination. These results have agreed well generally with prior methods of analysis and measured data taken on the large variety of spirals built through the years. One very useful insight in these analyses is the calculated currents on the wire segments. By plotting the current magnitudes versus the total arm length, the region where radiation occurs can be plainly seen, along with the current standing wave ratio (SWR) at the arm end that results from a non-optimum load. Detailed knowledge of these facts helps the antenna designer correct the design to meet the performance requirements.

In the designs attempted this year on electrically small spirals, MOM analyses were done to acquire some understanding of the problems that were going to be encountered. Prior experience with a narrower band "current" type antenna has shown that knowledge of the input impedance and radiation properties is critical to producing a successful design. Some knowledge of similar problems in the case of the spiral antenna will help avoid delays in getting a working design.

BASIC DESIGN CONCERNS OF ELECTRICALLY SMALL SPIRALS

The typical spiral design of the past has been done with the physical space allowed for it being used as the defining parameter for the low-frequency performance. In the standard approach, the Archimedean spiral geometry and its basic operation can be defined by a simple set of equations.

The geometry is based on a spatial complementary approach that provides for the spaces between the arms to be equal to the arm widths. For a given "N" arm spiral, the radius to any given point on the arm at a rotation angle θ is

$$R = a*\theta, \text{ where } a = \frac{N*W}{\pi} \text{ , w being the desired arm width}$$

For the Mth mode, the radiating region's circumference is defined as

$$C = 2*\pi*R, \text{ which is set equal to M times the wavelength } (\lambda)$$

Thus giving $R = \frac{M*\lambda}{(2*\pi)}$ for the radius of the radiating circumference.

These are the equations that have been used for years, and are based on the radiating ring model mentioned previously. For a real-life spiral, the actual arm length needs to be calculated and the location of the proper spiral current phases derived from this.

For an Archimedean spiral of geometry $R = A*\theta$ and $n = 1$, the arm length from starting angle $\theta 1$ to end angle $\theta 2$ is given by

$$\int_{\theta 1}^{\theta 2} \frac{A}{2\left(\theta * \sqrt{\theta^2 + 1} + A * \ln\left(\theta + \sqrt{\theta^2 + 1}\right)\right)}$$

At any given radial point, the difference between the length of adjacent arms of a two-arm spiral is given by the arm length evaluated from θ to $\theta + \pi$ radian. By finding the radius where this difference is equal to $\frac{*\lambda}{2}$, the location of the center of the radiating region for the first mode is determined. This value is illustrated below as compared to the previous value of $\frac{\lambda}{(2*\pi)}$ for frequencies from 0.1 to 20 GHz for Mode 1.

Radius of Radiation Versus Frequency (GHz)
Nominal Arm Width of 0.04 Inch.

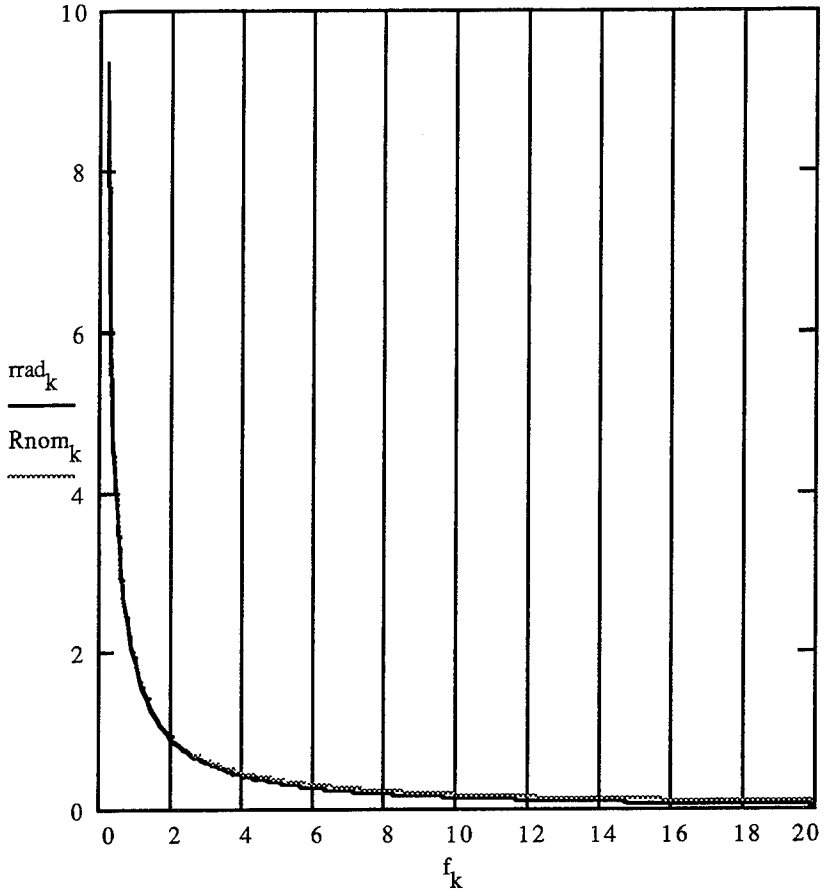

For the case shown these values are very close, differing appreciably only in cases of arm widths 0.10 inch wider or greater, at frequencies above 10 GHz. What is notable is the rapid increase in this radius for frequencies below 2 GHz. This rapid rise in needed aperture radius illustrates the fundamental problem of operating spiral antennas at frequencies below 2 GHz. The dimensions required for a conventional design increase very quickly as the frequency goes down.

What happens as the needed aperture becomes equal to the actual size of the antenna is the question mainly addressed in this report. The HTS spirals being built this year are considerably below this value. For a conventional spiral design, the diameter used for 500 MHz would be 7.5 inches. The spirals being built both here and at AEL are 3 inches in diameter. Although 1-inch-diameter spirals have been fabricated at AEL and operated below the conventional limits, the basic physics of the radiation model seems to indicate some large potential problems with apertures this small.

The basic requirement for the spiral to radiate is for the currents on the arms to become in phase at the proper diameter. This allows the radiated fields from the arm

currents to add together constructively in space, the basic condition for power transfer. For smaller diameters, these conditions are not met, and the sum of the radiated fields is very low. A rudimentary explanation of this situation follows.

For a spiral antenna to radiate, the adjacent arm currents must smoothly transition to an in-phase condition. This is normally attained by the gradual increasing difference in the arm lengths as explained above. The plot below illustrates this.

Phase of Adjacent Arms for Archimedean Spiral Arm
Width = 0.4 inch, 2 GHz.

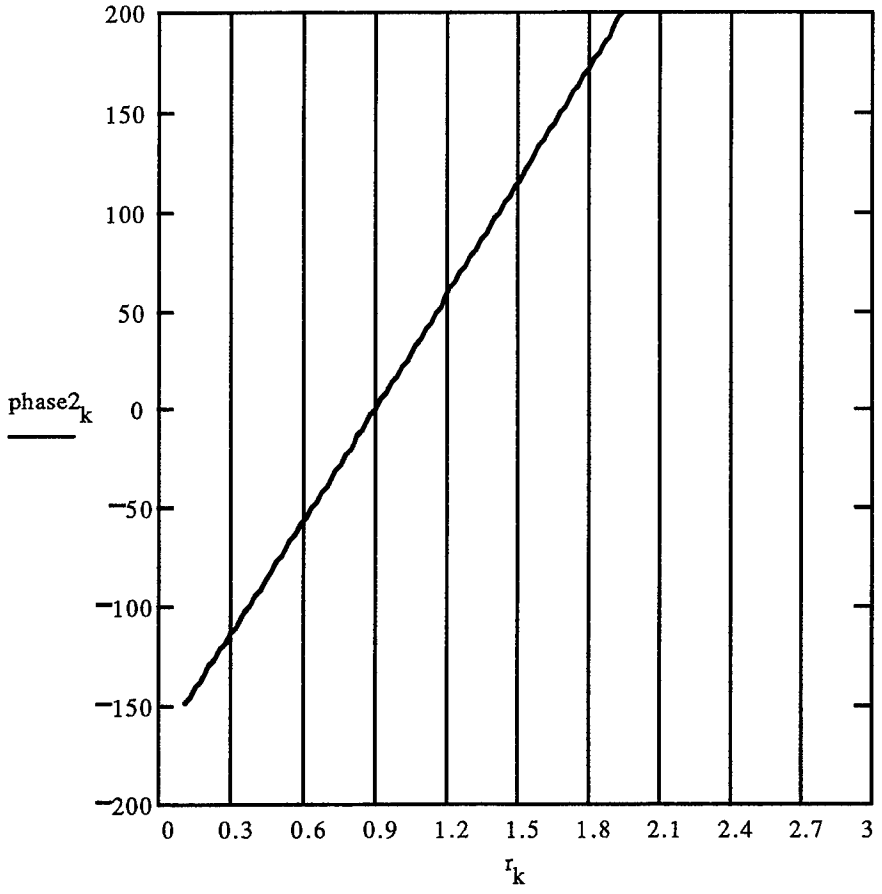

This plot shows the radius where the currents are in phase (the radiating region) being at 0.93 inch radius. The shape of the radiating region actually follows a Gaussian-type curve with respect to radius, which means for full gain the phase on the spiral needs to transition through about -90 up to +90 degrees. For this case, sufficient room for the entire radiation ring requires a 1.4-inch maximum radius.

The case for 0.5 GHz is illustrated below.

Phase of Adjacent Arms for Archimedean Spiral Arm Width = 0.4 Inch, 0.5 GHz.

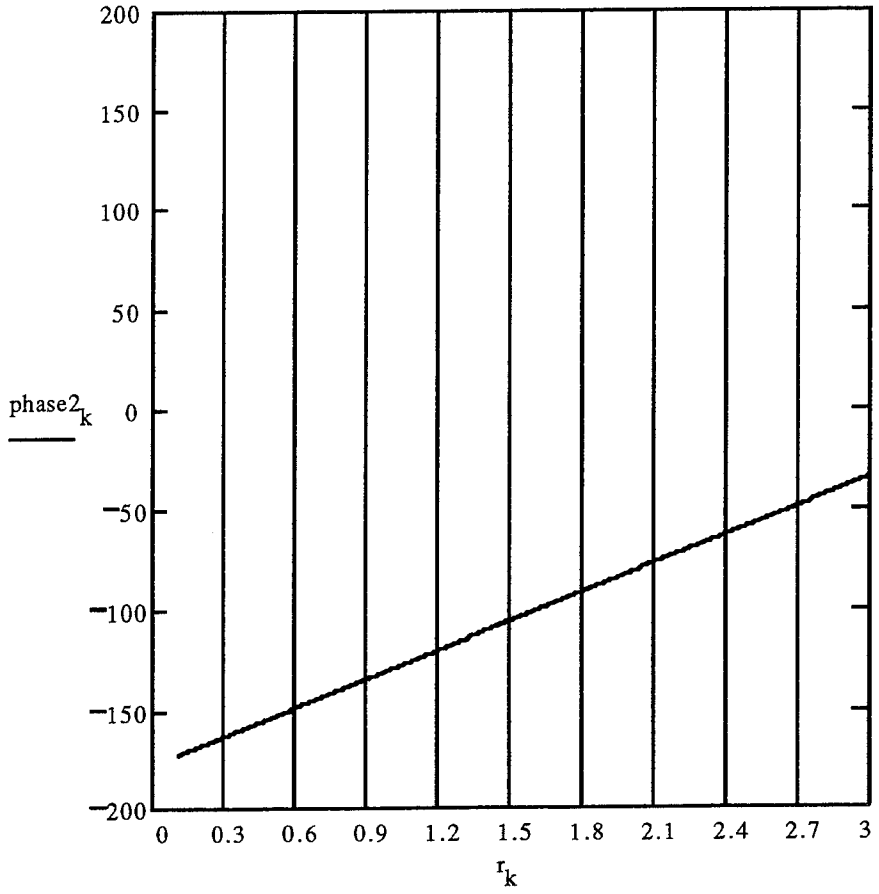

In this case, with a maximum antenna radius of 1.5 inches, the phase of the arms never reaches even the lower limit of -90 degrees. Thus, little radiation would be expected to occur. This briefly illustrates the current understanding of the radiation mechanism of spiral antennas and why radiation is difficult to obtain at frequencies below what the physical aperture will support. The main effects of low-frequency operation are a rapid decrease in gain, rapid degradation of the quality of circular polarization, adverse changes in input impedance, and increased sensitivity to the arm loading. It is due to these concerns that a MOM study of the spiral currents and radiating qualities at low frequencies has been done.

METHOD OF MOMENT ANALYIS

At the beginning of the project, analysis of the antenna was attempted using the GEMACS antenna analysis code (Reference 3) with the object of determining the best arm

loading impedance to use for the spiral being planned. The spiral arms were approximated with a series of wire segments following the Archimedean curve, with the last segment on each arm containing an arbitrary impedance and the end segments of the two arms connected together to approximate a ground contact. Two values of load impedance were used, 50 and 150 ohms. It was hoped that by varying the impedance around 100 ohms, that a value best suited to the frequencies intended for use would be found. The analysis included evaluating the input impedance and the spiral arm currents, and plotting the field pattern shape. The spiral diameter was fixed at 3 inches and the frequencies varied from 1.4 down to 0.5 GHz. These results were compared to the results for the same spiral with the arms open circuited (analyzed from 1.6 to 0.5 GHz). These results were expected to yield some insight into the arm load values needed. These analysis results are shown in Appendix A. After considerable time expended in running the analysis, the decision was made to limit the data examined to plots of the currents on the arms and the input impedance.

By examining the arm currents for the two loads used versus the open circuited spiral, it can be seen that neither value provides a match improvement across the frequency band. A good standard to compare to is the plot of the open circuited spiral at 1.6 GHz. The curve should be smooth, indicating small reflections at the arm ends. As the frequency goes down, the place where the current magnitude begins to drop should move toward the end of the arm, but if it is properly matched the curve should remain smooth. As is seen, the trend is for the currents to become more oscillating as the frequency drops, and the minimums to come closer to 0. This is an indication of a non-radiating open circuited line.

If the arms were loaded with an impedance matching the arm impedance at the end, the current curves plotted might not retain the same peak magnitude, but would be smooth, indicating no reflected currents. For the two cases tried, there was the trend for the loads to improve the match down to 1.1 GHz, with small improvement down to 0.8 GHz. The input impedance varied largely below 1.1 GHz. Thus, the simple approach used in the past proved to fail in this case. In fact, after many similar trials with other values of load impedance, none were found that would provide a good match over anything but narrow frequency bands.

SPIRAL IMPEDANCE ANALYSIS METHOD

After these attempts at finding simple resistive loads to match the spiral arms failed, it became obvious that the electrically small spiral presented a new problem. The impedance was not frequency independent any more, and was also a complex value. This began a search for methods to analyze the problem more rigorously. One method suggested was to characterize the spiral as a four-port device and then calculate the loads required to match at the arm ends. This was attempted with the help of a "Z" matrix calculation. By analyzing the spiral at the center terminals and then at the arm ends, these values were substituted into the calculation for the "Z" values to find the optimum load for maximum power transfer to the load. This should minimize the SWR of the current on the arms. A trial of this method was run at 800 MHz. The currents resulting from the load values obtained still seemed to have a high SWR. This method seemed to have promise, with further work still needed. During the course of these attempts, it was realized that the currents being derived in these

analysis were analogous to currents in a mismatched transmission line. By using the decades-old SWR matching technique, the optimum load value can be found (Reference 4).

The technique is fairly straightforward. By examining the SWR of the current or voltage at the end of the transmission line, the standing wave can be seen to be either at or between peaks. A mismatch in the imaginary part of the impedance will cause the wave to have a phase shift, resulting in a non-peak value at the end. By running the analysis with varied values for the imaginary part of the load, the wave will be at a peak when the spiral arms imaginary part is conjugate matched. By then looking at the SWR ratio after the arm is conjugate matched, the real part of the load impedance can be calculated. When the spiral arm is then loaded with this value, the current SWR should be minimized. This approach was used to find the optimum load values for the spiral model used at frequencies of 500 to 1100 MHz. The plot of real and imaginary parts of these load values and resultant input impedance is contained in Appendix B, along with an example of the improvement in current SWR at 800 MHz. These values were found to be predictable along a smooth curve up to 1200 MHz. At this frequency, the optimum load match values changed rapidly, and in fact could not be determined. It is believed that this may be a region where the spiral is operating between the electrically small case and the frequency indepedent case.

The load values obtained indicate a similar case to other electrically small antennas. The impedance real part rises with frequency and the imaginary part becomes more negative with increasing frequency, although it appears to be asymptotic to -100 ohms reactive.

These values are planned to be used as standards of comparison for other more rigorous methods in the future. Being analytically proven to be close to the optimum, other methods used should yield similar values. This was one problem with the analysis mentioned previously using the antenna four-port "Z" matrix. When it was compared to the values calculated using the slotted line type method, the values did not agree.

CONCLUSIONS

The electrically small spiral is a special case of the frequency independent spiral, with very different operating conditions and criterion. Much more analyses and experimentation needs to be done, considering the potential payoff in benefits to the military community. The reduced size spiral has been attempted with minute success for the last 30 years. The application of HTS materials to the problem promises to yield an improvement in size factor on the order of at least 2. Along these lines, further analyses can provide more insight into the operating characteristics of these devices. By performing more analysis and examining these analysis more deeply along with the test data on the hardware being built and due to be tested next fiscal year, the antenna performance should be further improved. Due to the present expensive nature of HTS circuits, these analyses could prove to be a large cost savings.

REFERENCES

1. Richard C. Johnson, ed. *Antenna Engineering Handbook.* New York, McGraw-Hill. Pp. 14-1-14-68.

2. Hisamatsu Nakano. *Helical and Sprial Antennas-A Numerical Approach.* New York, John Wiley & Sons, Inc.

3. Rome Air Development Center. *General Electromagnetic Model for the Analysis of Complex Systems*, by Edgar L. Coffey, Nancy W. Coffey, Diane L. Kadlec. Rome, New York, RADC, (RADC-TR-90-360, Vols. 1-3, available to DOD agencies only).

4. Harry E. Thomas. *Handbook of Microwave Techniques and Equipment.* New York, Prentice Hall. Pp. 183-185.

Appendix A

GEMACS SPIRAL ANALYSIS
OPEN CIRCUITED AND RESISTIVE TERMINATIONS

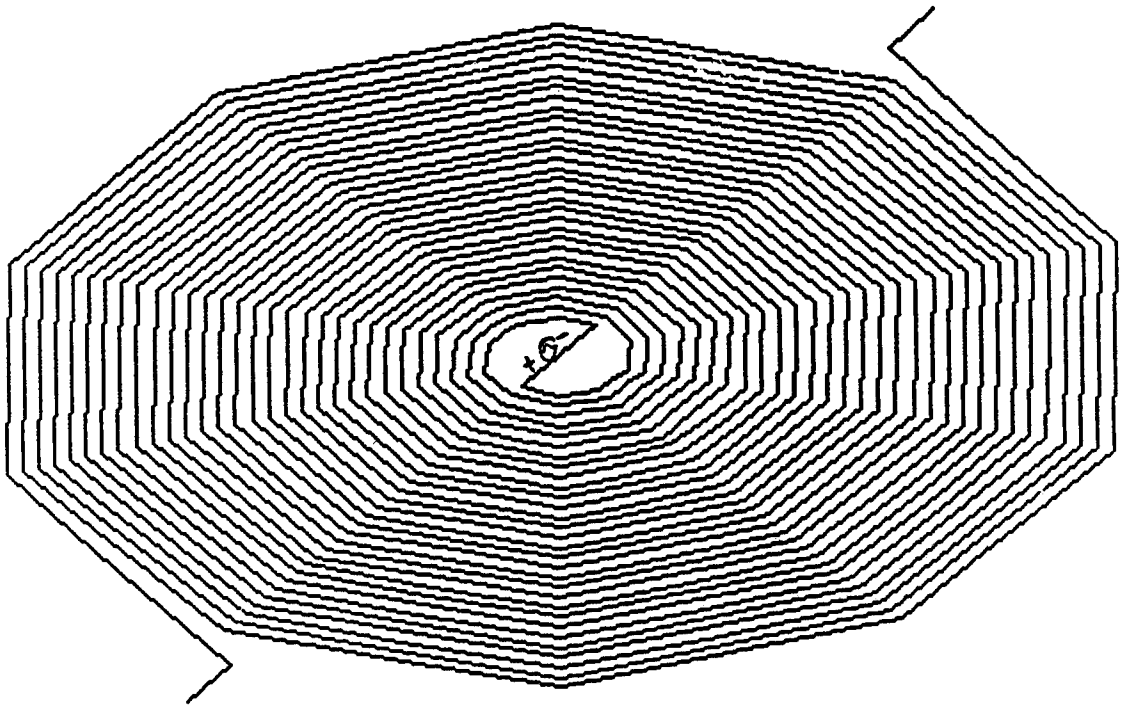

FIGURE A-1. Open Circuited Spiral Model.

GEMACS GEOMETRY FILE OPEN CIRCUITED SPIRAL

```
$
$ ARCHIMEDIAN SPIRAL ANTENNA
$
$ Requires: INPUT, MOM, SOLN, OUTPUT Modules
$
$ Estimated run time (i486SLC/20 w/coprocessor):
$
$  INPUT:  15.43 sec
$    MOM:  265.67
$   SOLN:  142.20
$ OUTPUT:  33.51
$-----------------------------------------------------------------
$
DISPLA ON LU=0
NUMFIL = 17
TIME = 10000.
SETINT MOM
$
$
FRQ =900
GMDATA = SPIRAL
$LOOP 1 8
DRIVE = VSRC(SPIRAL) V=1.,0. SEGS = 1
DRIVE = VSRC(SPIRAL) V=-1.,0. SEGS = 304
$ZLOADS=TERM GMDATA=SPIRAL prlc=1e5,.0318e-3,3.18e-6 SEGS=152,304
ZGEN GMDATA = SPIRAL ZMATRX = ZDIP   $ZLOADS=TERM
SOLVE ZDIP * I = DRIVE
PRINT module=soln I
$FLD = EFIELD(I)  P1=0.  T1=0.  DT=2.5 T2=180.
$FRQ=FRQ-100
$LABEL 1
END
$
$-----------------------------------------------------------
$ GEOMETRY FOR AN ARCHIMEDEAN SPIRAL ANTENNA
$
$ GENERATED ON: 11-13-87
$
$
$ TURNS PER INCH:   1.1000000E+01
$ TOTAL TURNS:     15
$ INNER RADIUS(In):  1.4000000E-01
$ SEGS PER TURN:   10
$ WIRE RADIUS(In):  1.0000000E-02
$ TOTAL DIAMETER:   2.7272730E+00
$
$ MAX SEG LENGTH(In):   9.4057550E-01
$ FREQ. LIMIT(MHZ):     1.2557200E+03  FOR LAMBDA/10 MODELING
$
$
$ THE ANTENNA SHOULD BE DRIVEN WITH +0.5 VOLTS ON SEGMENT 1
$                      AND -0.5 VOLTS ON SEGMENT 152
$-----------------------------------------------------------
$
SC IN   $UNITS PRESUMED TO BE INCHES IN INPUT DATA
RA  .01  .02
```

```
$ DRIVE SEGMENT# 1
WR 0. 0. 0. 4.0468000E-02 -1.5761510E-01 0. 2 1 1
$
$ BELOW ARE SEGMENTS 3 TO 22
$
WR 4.0468150E-02 -1.5761500E-01 0. 1.3238790E-01 -1.0952140E-01 0. 2 1 1
WR 1.3238790E-01 -1.0952140E-01 0. 1.8055210E-01 -1.1359840E-02 0. 2 1 1
WR 1.8055210E-01 -1.1359840E-02 0. 1.6042260E-01 1.0180680E-01 0. 2 1 1
WR 1.6042260E-01 1.0180680E-01 0. 7.3290640E-02 1.8510990E-01 0. 2 1 1
WR 7.3290640E-02 1.8510990E-01 0. -5.1772370E-02 2.0164150E-01 0. 2 1 1
WR -5.1772370E-02 2.0164150E-01 0. -1.6741140E-01 1.3849510E-01 0. 2 1 1
WR -1.6741140E-01 1.3849510E-01 0. -2.2591700E-01 1.4213780E-02 0. 2 1 1
WR -2.2591700E-01 1.4213780E-02 0. -1.9880100E-01 -1.2616270E-01 0. 2 1 1
WR -1.9880100E-01 -1.2616270E-01 0. -9.0023390E-02 -2.2737260E-01 0. 2 1 1
WR -9.0023390E-02 -2.2737260E-01 0. 6.3076700E-02 -2.4566800E-01 0. 2 1 1
$
$ BELOW ARE SEGMENTS 23 TO 42
$
WR 6.3076700E-02 -2.4566800E-01 0. 2.0243490E-01 -1.6746880E-01 0. 2 1 1
WR 2.0243490E-01 -1.6746880E-01 0. 2.7128190E-01 -1.7067610E-02 0. 2 1 1
WR 2.7128190E-01 -1.7067610E-02 0. 2.3717940E-01 1.5051870E-01 0. 2 1 1
WR 2.3717940E-01 1.5051870E-01 0. 1.0675600E-01 2.6963530E-01 0. 2 1 1
WR 1.0675600E-01 2.6963530E-01 0. -7.4381140E-02 2.8969450E-01 0. 2 1 1
WR -7.4381140E-02 2.8969450E-01 0. -2.3745850E-01 1.9644230E-01 0. 2 1 1
WR -2.3745850E-01 1.9644230E-01 0. -3.1664680E-01 1.9921320E-02 0. 2 1 1
WR -3.1664680E-01 1.9921320E-02 0. -2.7555780E-01 -1.7487490E-01 0. 2 1 1
WR -2.7555780E-01 -1.7487490E-01 0. -1.2348860E-01 -3.1189810E-01 0. 2 1 1
WR -1.2348860E-01 -3.1189810E-01 0. 8.5685690E-02 -3.3372090E-01 0. 2 1 1
$
$ BELOW ARE SEGMENTS 43 TO 62
$
WR 8.5685690E-02 -3.3372090E-01 0. 2.7248220E-01 -2.2541580E-01 0. 2 1 1
WR 2.7248220E-01 -2.2541580E-01 0. 3.6201170E-01 -2.2774910E-02 0. 2 1 1
WR 3.6201170E-01 -2.2774910E-02 0. 3.1393610E-01 1.9923110E-01 0. 2 1 1
WR 3.1393610E-01 1.9923110E-01 0. 1.4022100E-01 3.5416090E-01 0. 2 1 1
WR 1.4022100E-01 3.5416090E-01 0. -9.6990370E-02 3.7774730E-01 0. 2 1 1
WR -9.6990370E-02 3.7774730E-01 0. -3.0750590E-01 2.5438910E-01 0. 2 1 1
WR -3.0750590E-01 2.5438910E-01 0. -4.0737670E-01 2.5628390E-02 0. 2 1 1
WR -4.0737670E-01 2.5628390E-02 0. -3.5231430E-01 -2.2358750E-01 0. 2 1 1
WR -3.5231430E-01 -2.2358750E-01 0. -1.5695330E-01 -3.9642380E-01 0. 2 1 1
WR -1.5695330E-01 -3.9642380E-01 0. 1.0829520E-01 -4.2177360E-01 0. 2 1 1
$
$ BELOW ARE SEGMENTS 63 TO 82
$
WR 1.0829520E-01 -4.2177360E-01 0. 3.4252970E-01 -2.8336240E-01 0. 2 1 1
WR 3.4252970E-01 -2.8336240E-01 0. 4.5274160E-01 -2.8481750E-02 0. 2 1 1
WR 4.5274160E-01 -2.8481750E-02 0. 3.9069240E-01 2.4794390E-01 0. 2 1 1
WR 3.9069240E-01 2.4794390E-01 0. 1.7368550E-01 4.3868670E-01 0. 2 1 1
WR 1.7368550E-01 4.3868670E-01 0. -1.1960000E-01 4.6580000E-01 0. 2 1 1
WR -1.1960000E-01 4.6580000E-01 0. -3.7755360E-01 3.1233560E-01 0. 2 1 1
WR -3.7755360E-01 3.1233560E-01 0. -4.9810650E-01 3.1335000E-02 0. 2 1 1
WR -4.9810650E-01 3.1335000E-02 0. -4.2907050E-01 -2.7230050E-01 0. 2 1 1
WR -4.2907050E-01 -2.7230050E-01 0. -1.9041760E-01 -4.8094960E-01 0. 2 1 1
WR -1.9041760E-01 -4.8094960E-01 0. 1.3090500E-01 -5.0982630E-01 0. 2 1 1
$
$ BELOW ARE SEGMENTS 83 TO 102
```

```
$
WR  1.3090500E-01 -5.0982630E-01 0.  4.1257760E-01 -3.4130870E-01 0.  2 1 1
WR  4.1257760E-01 -3.4130870E-01 0.  5.4347150E-01 -3.4188130E-02 0.  2 1 1
WR  5.4347150E-01 -3.4188130E-02 0.  4.6744850E-01  2.9665710E-01 0.  2 1 1
WR  4.6744850E-01  2.9665710E-01 0.  2.0714950E-01  5.2321260E-01 0.  2 1 1
WR  2.0714950E-01  5.2321260E-01 0. -1.4221020E-01  5.5385260E-01 0.  2 1 1
WR -1.4221020E-01  5.5385260E-01 0. -4.4760160E-01  3.7028170E-01 0.  2 1 1
WR -4.4760160E-01  3.7028170E-01 0. -5.8883640E-01  3.7041140E-02 0.  2 1 1
WR -5.8883640E-01  3.7041140E-02 0. -5.0582650E-01 -3.2101380E-01 0.  2 1 1
WR -5.0582650E-01 -3.2101380E-01 0. -2.2388140E-01 -5.6547560E-01 0.  2 1 1
WR -2.2388140E-01 -5.6547560E-01 0.  1.5351540E-01 -5.9787880E-01 0.  2 1 1
$
$ BELOW ARE SEGMENTS 103 TO 122
$
WR  1.5351540E-01 -5.9787880E-01 0.  4.8262580E-01 -3.9925460E-01 0.  2 1 1
WR  4.8262580E-01 -3.9925460E-01 0.  6.3420140E-01 -3.9894040E-02 0.  2 1 1
WR  6.3420140E-01 -3.9894040E-02 0.  5.4420440E-01  3.4537070E-01 0.  2 1 1
WR  5.4420440E-01  3.4537070E-01 0.  2.4061320E-01  6.0773870E-01 0.  2 1 1
WR  2.4061320E-01  6.0773870E-01 0. -1.6482070E-01  6.4190500E-01 0.  2 1 1
WR -1.6482070E-01  6.4190500E-01 0. -5.1765000E-01  4.2822750E-01 0.  2 1 1
WR -5.1765000E-01  4.2822750E-01 0. -6.7956640E-01  4.2746820E-02 0.  2 1 1
WR -6.7956640E-01  4.2746820E-02 0. -5.8258220E-01 -3.6972760E-01 0.  2 1 1
WR -5.8258220E-01 -3.6972760E-01 0. -2.5734480E-01 -6.5000180E-01 0.  2 1 1
WR -2.5734480E-01 -6.5000180E-01 0.  1.7612620E-01 -6.8593130E-01 0.  2 1 1
$
$ BELOW ARE SEGMENTS 123 TO 142
$
WR  1.7612620E-01 -6.8593130E-01 0.  5.5267420E-01 -4.5720020E-01 0.  2 1 1
WR  5.5267420E-01 -4.5720020E-01 0.  7.2493130E-01 -4.5599490E-02 0.  2 1 1
WR  7.2493130E-01 -4.5599490E-02 0.  6.2096000E-01  3.9408460E-01 0.  2 1 1
WR  6.2096000E-01  3.9408460E-01 0.  2.7407640E-01  6.9226500E-01 0.  2 1 1
WR  2.7407640E-01  6.9226500E-01 0. -1.8743180E-01  7.2995740E-01 0.  2 1 1
WR -1.8743180E-01  7.2995740E-01 0. -5.8769850E-01  4.8617280E-01 0.  2 1 1
WR -5.8769850E-01  4.8617280E-01 0. -7.7029630E-01  4.8452040E-02 0.  2 1 1
WR -7.7029630E-01  4.8452040E-02 0. -6.5933780E-01 -4.1844170E-01 0.  2 1 1
WR -6.5933780E-01 -4.1844170E-01 0. -2.9080790E-01 -7.3452810E-01 0.  2 1 1
WR -2.9080790E-01 -7.3452810E-01 0.  1.9873750E-01 -7.7398350E-01 0.  2 1 1
$
$ BELOW ARE SEGMENTS 143 TO 162
$
WR  1.9873750E-01 -7.7398350E-01 0.  6.2272300E-01 -5.1514540E-01 0.  2 1 1
WR  6.2272300E-01 -5.1514540E-01 0.  8.1566130E-01 -5.1304470E-02 0.  2 1 1
WR  8.1566130E-01 -5.1304470E-02 0.  6.9771540E-01  4.4279890E-01 0.  2 1 1
WR  6.9771540E-01  4.4279890E-01 0.  3.0753920E-01  7.7679130E-01 0.  2 1 1
WR  3.0753920E-01  7.7679130E-01 0. -2.1004320E-01  8.1800960E-01 0.  2 1 1
WR -2.1004320E-01  8.1800960E-01 0. -6.5774740E-01  5.4411790E-01 0.  2 1 1
WR -6.5774740E-01  5.4411790E-01 0. -8.6102630E-01  5.4156790E-02 0.  2 1 1
WR -8.6102630E-01  5.4156790E-02 0. -7.3609300E-01 -4.6715630E-01 0.  2 1 1
WR -7.3609300E-01 -4.6715630E-01 0. -3.2427040E-01 -8.1905470E-01 0.  2 1 1
WR -3.2427040E-01 -8.1905470E-01 0.  2.2134920E-01 -8.6203570E-01 0.  2 1 1
$
$ BELOW ARE SEGMENTS 82 TO 182
$
WR  2.2134920E-01 -8.6203570E-01 0.  6.9277200E-01 -5.7309020E-01 0.  2 1 1
WR  6.9277200E-01 -5.7309020E-01 0.  9.0639130E-01 -5.7008990E-02 0.  2 1 1
WR  9.0639130E-01 -5.7008990E-02 0.  7.7447050E-01  4.9151380E-01 0.  2 1 1
```

```
WR 7.7447050E-01 4.9151380E-01 0. 3.4100480E-01 8.6131660E-01 0. 2 1 1
WR 3.4100480E-01 8.6131660E-01 0. -2.3265170E-01 9.0606260E-01 0. 2 1 1
WR -2.3265170E-01 9.0606260E-01 0. -7.2779430E-01 6.0206530E-01 0. 2 1 1
WR -7.2779430E-01 6.0206530E-01 0. -9.5175610E-01 5.9864700E-02 0. 2 1 1
WR -9.5175610E-01 5.9864700E-02 0. -8.1284990E-01 -5.1586810E-01 0. 2 1 1
WR -8.1284990E-01 -5.1586810E-01 0. -3.5773600E-01 -9.0357990E-01 0. 2 1 1
WR -3.5773600E-01 -9.0357990E-01 0. 2.4395770E-01 -9.5008870E-01 0. 2 1 1
$
$ BELOW ARE SEGMENTS 92 TO 202
$
WR 2.4395770E-01 -9.5008870E-01 0. 7.6281890E-01 -6.3103770E-01 0. 2 1 1
WR 7.6281890E-01 -6.3103770E-01 0. 9.9712110E-01 -6.2716850E-02 0. 2 1 1
WR 9.9712110E-01 -6.2716850E-02 0. 8.5122740E-01 5.4022560E-01 0. 2 1 1
WR 8.5122740E-01 5.4022560E-01 0. 3.7446700E-01 9.4584320E-01 0. 2 1 1
WR 3.7446700E-01 9.4584320E-01 0. -2.5526370E-01 9.9411460E-01 0. 2 1 1
WR -2.5526370E-01 9.9411460E-01 0. -7.9784360E-01 6.6000990E-01 0. 2 1 1
WR -7.9784360E-01 6.6000990E-01 0. -1.0424860E+00 6.5568870E-02 0. 2 1 1
WR -1.0424860E+00 6.5568870E-02 0. -8.8960490E-01 -5.6458320E-01 0. 2 1 1
WR -8.8960490E-01 -5.6458320E-01 0. -3.9119800E-01 -9.8810670E-01 0. 2 1 1
WR -3.9119800E-01 -9.8810670E-01 0. 2.6656990E-01 -1.0381410E+00 0. 2 1 1
$
$ BELOW ARE SEGMENTS 102 TO 222
$
WR 2.6656990E-01 -1.0381410E+00 0. 8.3286830E-01 -6.8898200E-01 0. 2 1 1
WR 8.3286830E-01 -6.8898200E-01 0. 1.0878510E+00 -6.8420780E-02 0. 2 1 1
WR 1.0878510E+00 -6.8420780E-02 0. 9.2798220E-01 5.8894080E-01 0. 2 1 1
WR 9.2798220E-01 5.8894080E-01 0. 4.0792890E-01 1.0303700E+00 0. 2 1 1
WR 4.0792890E-01 1.0303700E+00 0. -2.7787630E-01 1.0821670E+00 0. 2 1 1
WR -2.7787630E-01 1.0821670E+00 0. -8.6789320E-01 7.1795410E-01 0. 2 1 1
WR -8.6789320E-01 7.1795410E-01 0. -1.1332160E+00 7.1272570E-02 0. 2 1 1
WR -1.1332160E+00 7.1272570E-02 0. -9.6635950E-01 -6.1329850E-01 0. 2 1 1
WR -9.6635950E-01 -6.1329850E-01 0. -4.2465960E-01 -1.0726340E+00 0. 2 1 1
WR -4.2465960E-01 -1.0726340E+00 0. 2.8918270E-01 -1.1261930E+00 0. 2 1 1
$
$ BELOW ARE SEGMENTS 112 TO 242
$
WR 2.8918270E-01 -1.1261930E+00 0. 9.0291810E-01 -7.4692610E-01 0. 2 1 1
WR 9.0291810E-01 -7.4692610E-01 0. 1.1785810E+00 -7.4124250E-02 0. 2 1 1
WR 1.1785810E+00 -7.4124250E-02 0. 1.0047370E+00 6.3765650E-01 0. 2 1 1
WR 1.0047370E+00 6.3765650E-01 0. 4.4139020E-01 1.1148970E+00 0. 2 1 1
WR 4.4139020E-01 1.1148970E+00 0. -3.0048920E-01 1.1702190E+00 0. 2 1 1
WR -3.0048920E-01 1.1702190E+00 0. -9.3794300E-01 7.7589790E-01 0. 2 1 1
WR -9.3794300E-01 7.7589790E-01 0. -1.2239460E+00 7.6975810E-02 0. 2 1 1
WR -1.2239460E+00 7.6975810E-02 0. -1.0431140E+00 -6.6201440E-01 0. 2 1 1
WR -1.0431140E+00 -6.6201440E-01 0. -4.5812070E-01 -1.1571610E+00 0. 2 1 1
WR -4.5812070E-01 -1.1571610E+00 0. 3.1179590E-01 -1.2142440E+00 0. 2 1 1
$
$ BELOW ARE SEGMENTS 122 TO 262
$
WR 3.1179590E-01 -1.2142440E+00 0. 9.7296810E-01 -8.0486970E-01 0. 2 1 1
WR 9.7296810E-01 -8.0486970E-01 0. 1.2693110E+00 -7.9827260E-02 0. 2 1 1
WR 1.2693110E+00 -7.9827260E-02 0. 1.0814910E+00 6.8637250E-01 0. 2 1 1
WR 1.0814910E+00 6.8637250E-01 0. 4.7485110E-01 1.1994240E+00 0. 2 1 1
WR 4.7485110E-01 1.1994240E+00 0. -3.2310260E-01 1.2582700E+00 0. 2 1 1
WR -3.2310260E-01 1.2582700E+00 0. -1.0079930E+00 8.3384140E-01 0. 2 1 1
WR -1.0079930E+00 8.3384140E-01 0. -1.3146760E+00 8.2678590E-02 0. 2 1 1
```

```
WR -1.3146760E+00  8.2678590E-02 0. -1.1198680E+00 -7.1073070E-01 0.  2 1 1
WR -1.1198680E+00 -7.1073070E-01 0. -4.9158140E-01 -1.2416880E+00 0.  2 1 1
WR -4.9158140E-01 -1.2416880E+00 0.  3.3440940E-01 -1.3022960E+00 0.  2 1 1
$
$ BELOW ARE SEGMENTS 132 TO 282
$
WR  3.3440940E-01 -1.3022960E+00 0.  1.0430180E+00 -8.6281300E-01 0.  2 1 1
WR  1.0430180E+00 -8.6281300E-01 0.  1.3600410E+00 -8.5529800E-02 0.  2 1 1
WR  1.3600410E+00 -8.5529800E-02 0.  1.1582450E+00  7.3508890E-01 0.  2 1 1
WR  1.1582450E+00  7.3508890E-01 0.  5.0831170E-01  1.2839520E+00 0.  2 1 1
WR  5.0831170E-01  1.2839520E+00 0. -3.4571640E-01  1.3463220E+00 0.  2 1 1
WR -3.4571640E-01  1.3463220E+00 0. -1.0780440E+00  8.9178460E-01 0.  2 1 1
WR -1.0780440E+00  8.9178460E-01 0. -1.4054060E+00  8.8380900E-02 0.  2 1 1
WR -1.4054060E+00  8.8380900E-02 0. -1.1966220E+00 -7.5944720E-01 0.  2 1 1
WR -1.1966220E+00 -7.5944720E-01 0. -5.2504180E-01 -1.3262150E+00 0.  2 1 1
WR -5.2504180E-01 -1.3262150E+00 0.  3.5702350E-01 -1.3903480E+00 0.  2 1 1
$
$ BELOW ARE SEGMENTS 142 TO 303
$actually now to 152
$
WR  3.5702350E-01 -1.3903480E+00 0.  1.1130690E+00 -9.2075590E-01 0.  2 1 1
WR  1.1130690E+00 -9.2075590E-01 0.  1.4507720E+00 -9.1231890E-02 0.  2 1 1
WR  1.4507720E+00 -9.1231890E-02 0.  1.2349990E+00  7.8380570E-01 0.  2 1 1
WR  1.2349990E+00  7.8380570E-01 0.  5.4177180E-01  1.3684790E+00 0.  2 1 1
WR  5.4177180E-01  1.3684790E+00 0. -3.6833070E-01  1.4343730E+00 0.  2 1 1
WR -3.6833070E-01  1.4343730E+00 0. -1.1480940E+00  9.4972740E-01 0.  2 1 1
WR -1.1480940E+00  9.4972740E-01 0. -1.4961370E+00  9.4082740E-02 0.  2 1 1
WR -1.4961370E+00  9.4082740E-02 0. -1.2733760E+00 -8.0816420E-01 0.  2 1 1
WR -1.2733760E+00 -8.0816420E-01 0. -5.5850160E-01 -1.4107430E+00 0.  2 1 1
WR -5.5850160E-01 -1.4107430E+00 0.  4.9440000E-01 -1.5216000E+00 0.  2 1 1
WR  .4944 -1.5216 0.  .5562 -1.719 0.  1 1 1
$******  one segment per wire= 1,151  ******
$  ROTATE ARM ONE TO GENERATE ARM TWO
$
$  SEGMENTS 304 TO 606
$******  one segment per wire= 152,304
RZ TG 1 1  180.
$RSYM 2
$PT 610 1.8 0. 0.
$RZ PT 610 1 18.
$PT 612 1.9 0. 0.
$RZ PT 612 1 18.
$DF RING
$CP 610 611 1 2 2
$CP 610 612 1 2 2
$CP 612 613 1 2 2
$RZ DF RING 9 18.
$DE
$RZ TG 2 1 180.
RSYM 2
END
```

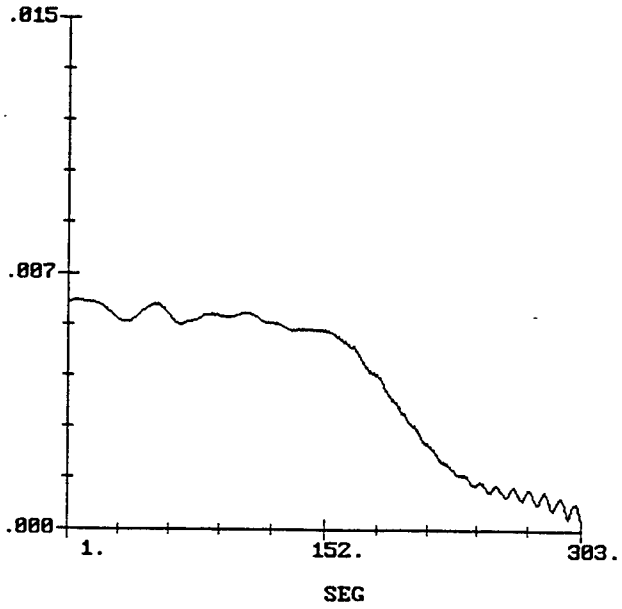

FIGURE A-2. 1.6-GHz Current Versus Arm Segment # Plot.

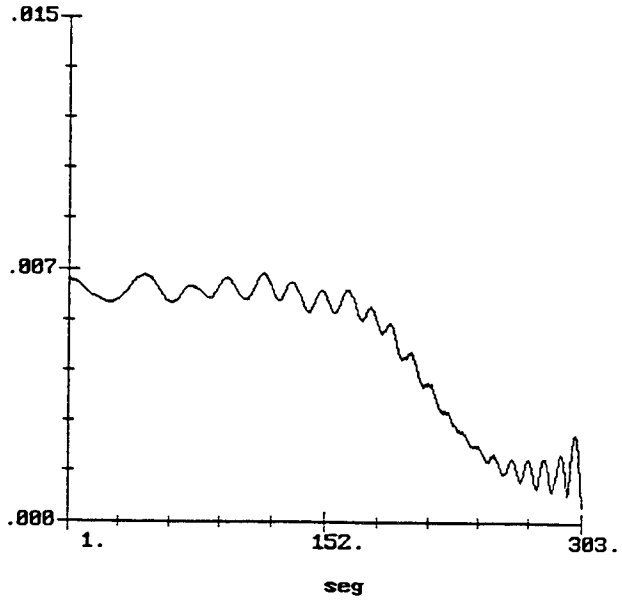

FIGURE A-3. 1.5-GHz Current Versus Arm Segment # Plot.

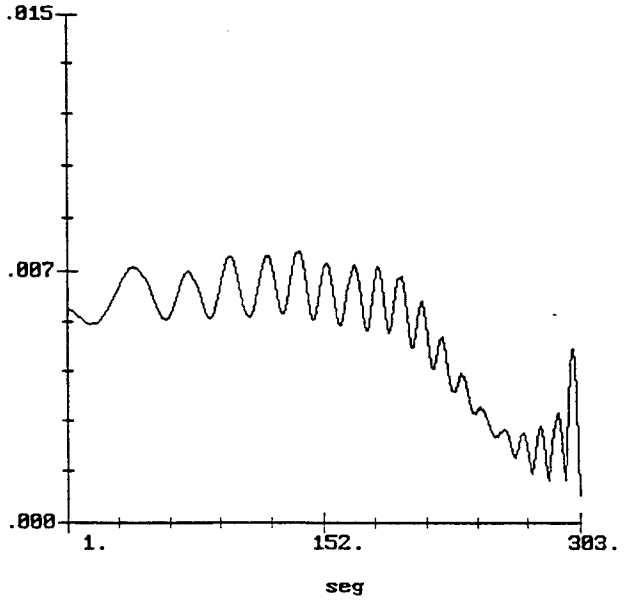

FIGURE A-4. 1.4-GHz Current Versus Arm Segment # Plot.

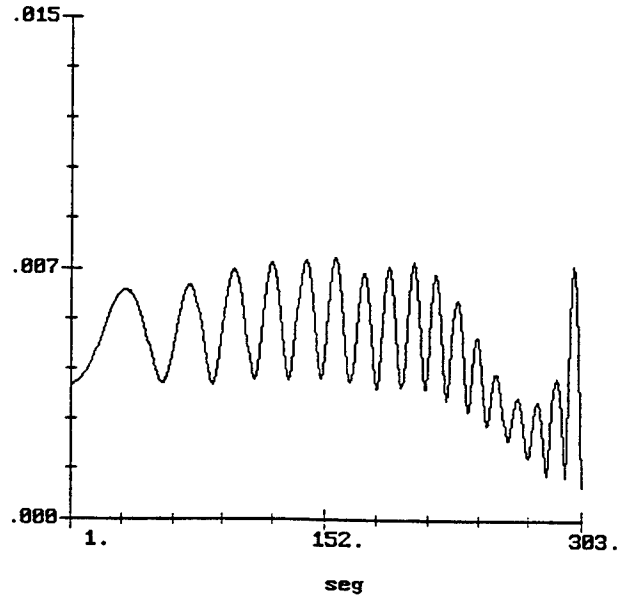

FIGURE A-5. 1.3-GHz Current Versus Arm Segment # Plot.

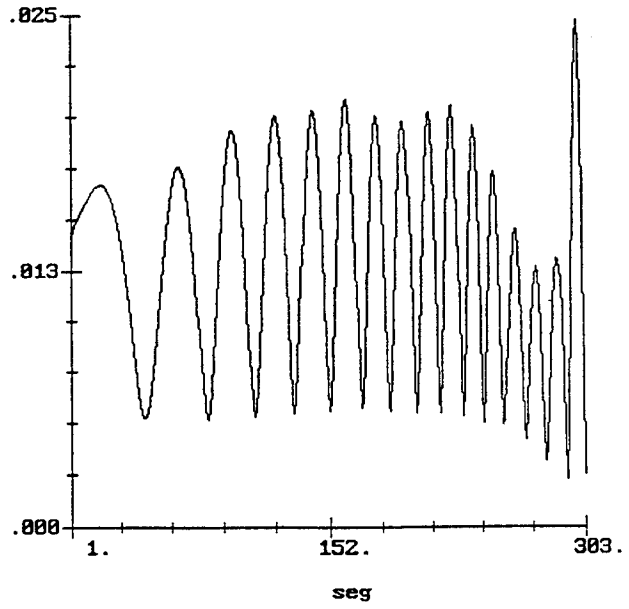

FIGURE A-6. 1.2-GHz Current Versus Arm Segment # Plot.

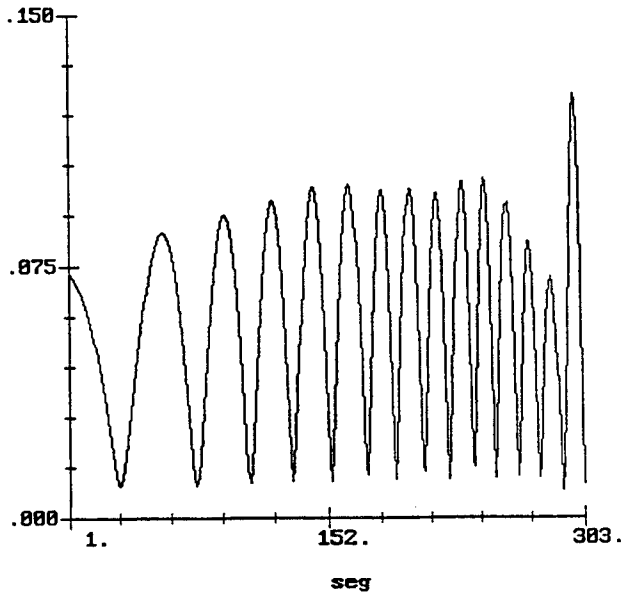

FIGURE A-7. 1.1-GHz Current Versus Arm Segment # Plot.

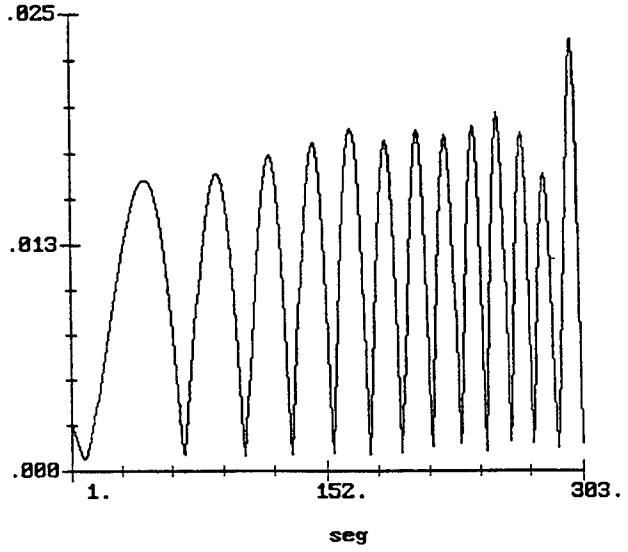

FIGURE A-8. 1.0-GHz Current Versus Arm Segment # Plot.

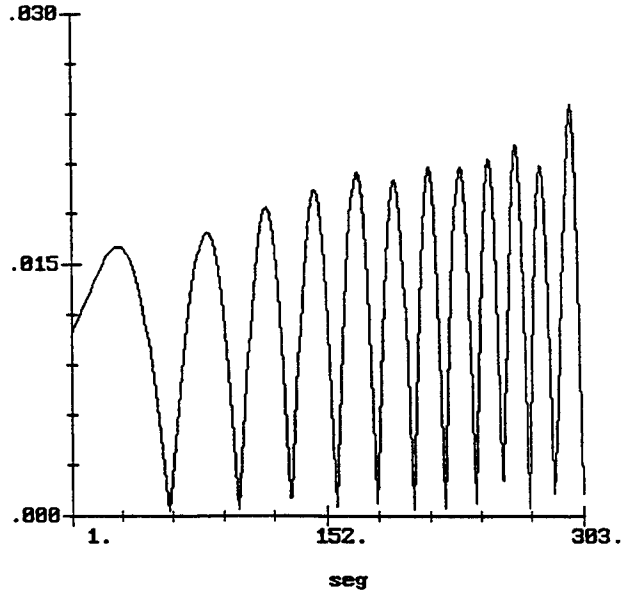

FIGURE A-9. 0.9-GHz Current Versus Arm Segment # Plot.

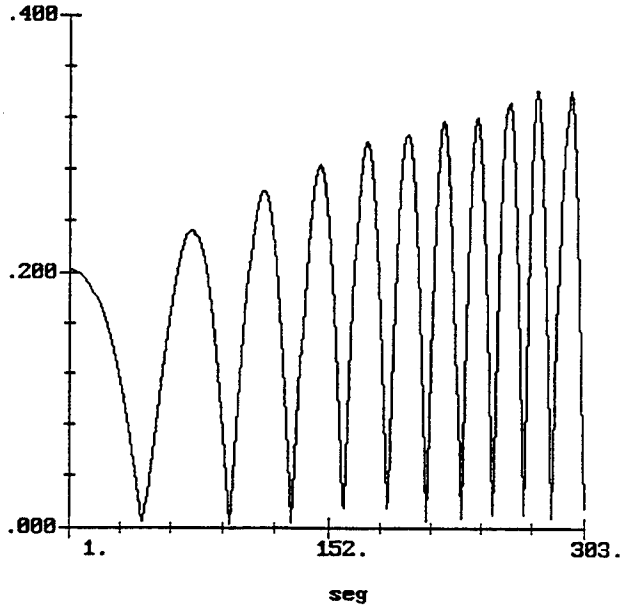

FIGURE A-10. 0.8-GHz Current Versus Arm Segment # Plot.

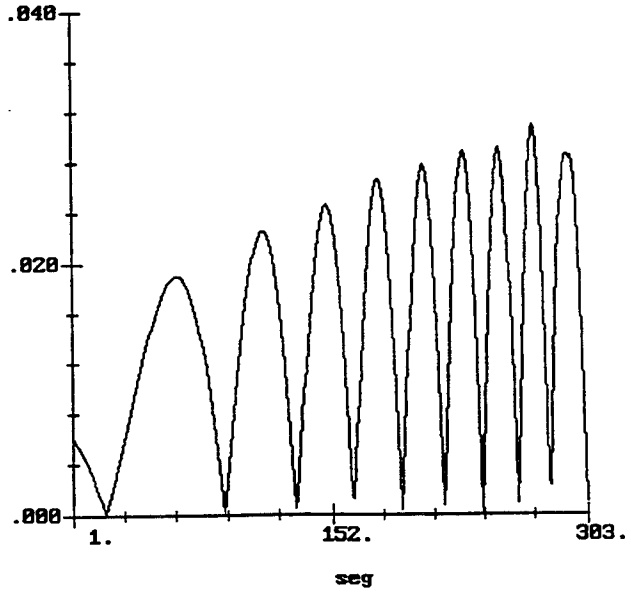

FIGURE A-11. 0.7-GHz Current Versus Arm Segment # Plot.

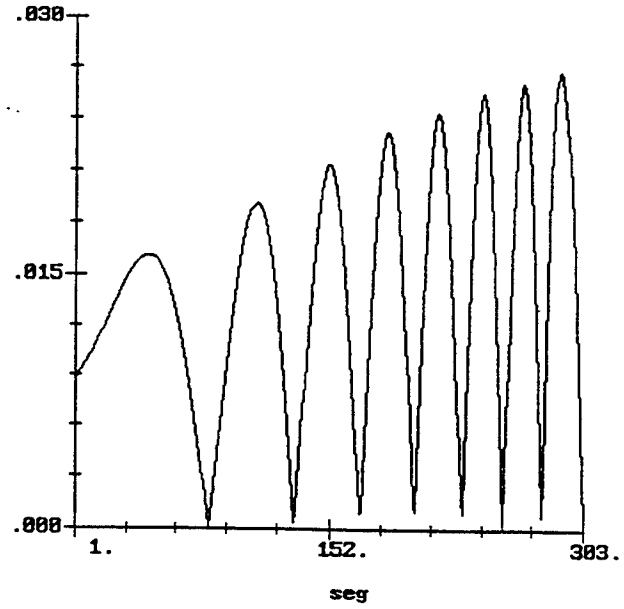

FIGURE A-12. 0.6-GHz Current Versus Arm Segment # Plot.

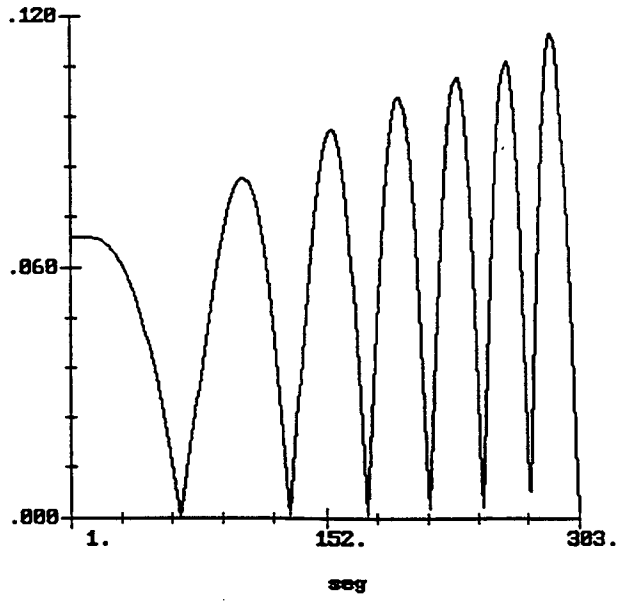

FIGURE A-13. 0.5-GHz Current Versus Arm Segment # Plot.

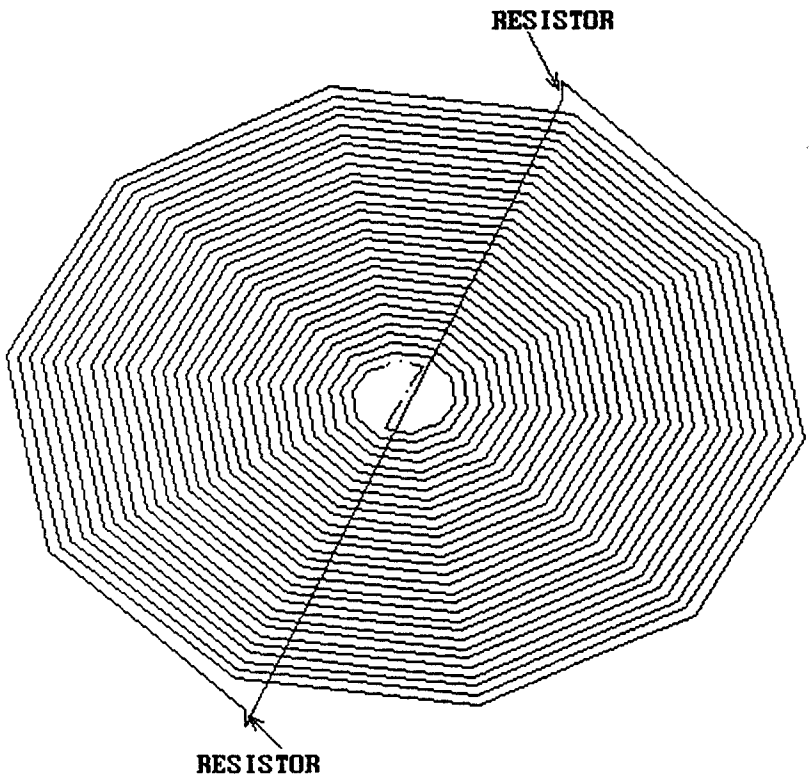

FIGURE A-14. Loaded Spiral Model.

GEMACS GEOMETRY FILE LOADED SPIRAL

```
$
$ ARCHIMEDIAN SPIRAL ANTENNA
$
$ Requires: INPUT, MOM, SOLN, OUTPUT Modules
$
$ Estimated run time (i486SLC/20 w/coprocessor):
$
$   INPUT:   15.43 sec
$     MOM:  265.67
$    SOLN:  142.20
$  OUTPUT:   33.51
$-------------------------------------------------------------------------
$
DISPLA ON LU=0
NUMFIL = 17
TIME = 10000.
SETINT MOM
$
$
FRQ =900.
GMDATA = SPIRAL
$LOOP 1 7
DRIVE = VSRC(SPIRAL) V=1.,0. SEGS = 1
DRIVE = VSRC(SPIRAL) V=-1.,0. SEGS = 304
ZLOADS=TERM GMDATA=SPIRAL ZIMP=50.,0. SEGS=303,306     $ ZIMP=150.,0. FOR SECOND
ZLOADS=TERM GMDATA=SPIRAL ZIMP=0.001,0. SEGS=607
ZEN GMDATA = SPIRAL ZMATRX = ZDIP   ZLOADS=TERM
SOLVE ZDIP * I = DRIVE
PRINT module=soln I
$FLD = EFIELD(I)  P1=0.  T1=0.  DT=2.5 T2=180.
$FRQ=FRQ+100
$LABEL 1
END
$
$-------------------------------------------------------------------------
$  GEOMETRY FOR AN ARCHIMEDEAN SPIRAL ANTENNA
$
$  GENERATED ON: 11-13-87
$
$
$  TURNS PER INCH:    1.1000000E+01
$  TOTAL TURNS:      15
$  INNER RADIUS(In):  1.4000000E-01
$  SEGS PER TURN:    10
$  WIRE RADIUS(In):   1.0000000E-02
$  TOTAL DIAMETER:    2.7272730E+00
$
$  MAX SEG LENGTH(In):    9.4057550E-01
$  FREQ. LIMIT(MHZ):      1.2557200E+03  FOR LAMBDA/10 MODELING
$
$
$  THE ANTENNA SHOULD BE DRIVEN WITH +0.5 VOLTS ON SEGMENT 1
$                                AND -0.5 VOLTS ON SEGMENT 152
$-------------------------------------------------------------------------
$ADDED TO SP2OPN.GEM WIRE DEFINITIONS
WR  .4944   -1.5216    -.0   .4944   1.5216    -.10  1 1 1
$******    one segment per wire= 1,151    ******
$  ROTATE ARM ONE TO GENERATE ARM TWO
$
$  SEGMENTS 304 TO 606

 $******   one segment per wire=  152,304
 RZ TG 1 1  180.
 RSYM 2
 WR  .4944   -1.5216    -.10   -.4944   1.5216    -.10  1 1 1
 END
```

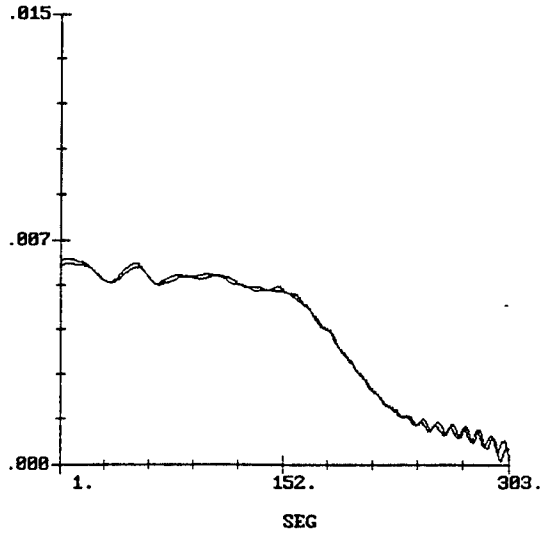

FIGURE A-15. 50-Ohm Load 1.6 GHz.

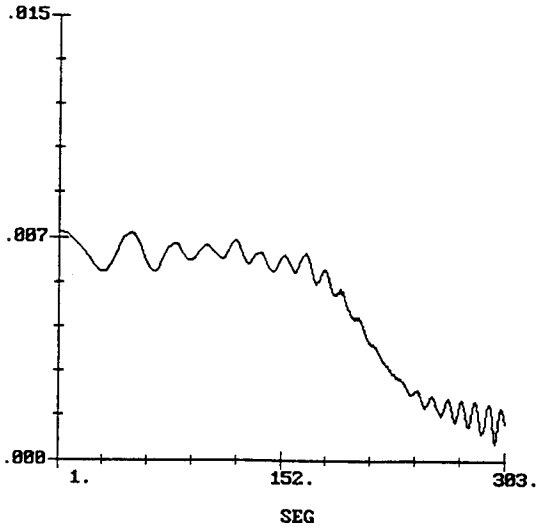

FIGURE A-16. 50-Ohm Load 1.5 GHz.

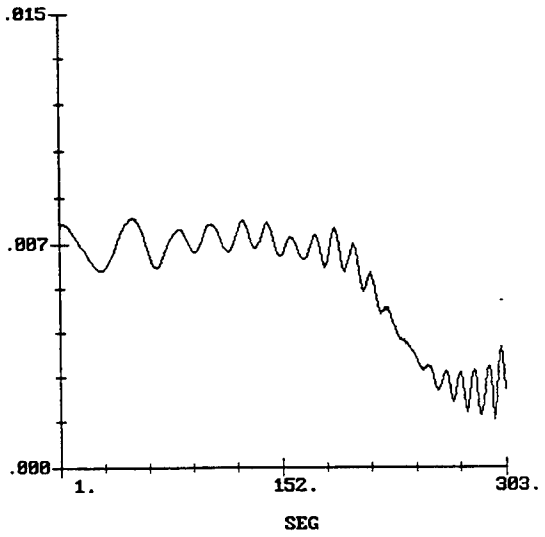

FIGURE A-17. 50-Ohm Load 1.4 GHz.

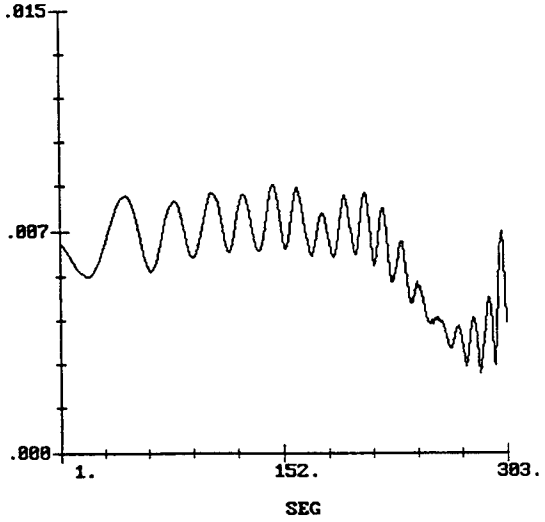

FIGURE A-18. 50-Ohm Load 1.3 GHz.

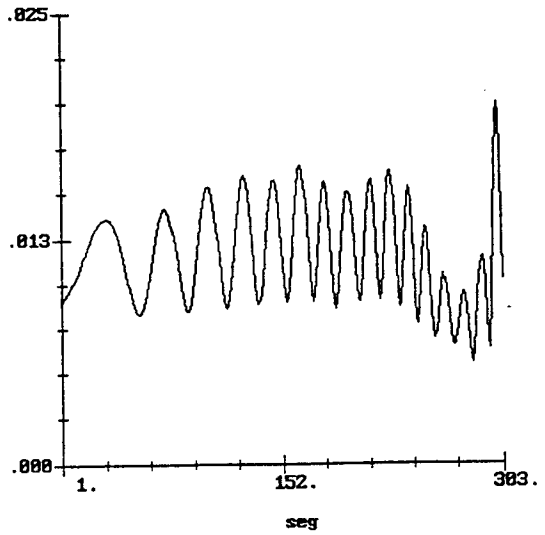

FIGURE A-19. 50-Ohm Load 1.2 GHz.

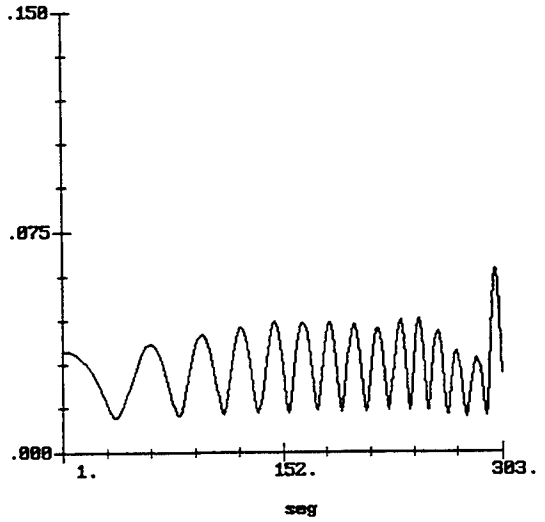

FIGURE A-20. 50-Ohm Load 1.1 GHz.

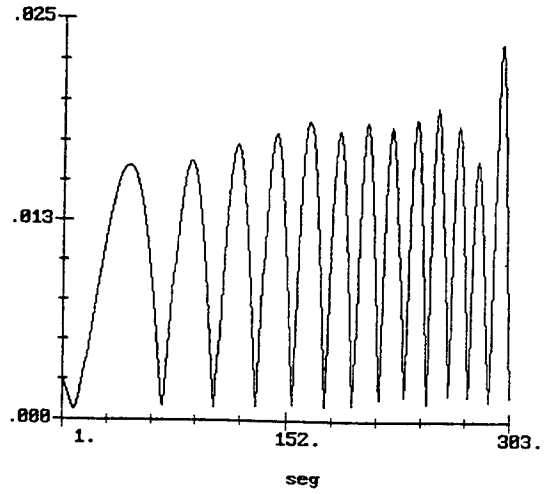

FIGURE A-21. 50-Ohm Load 1.0 GHz.

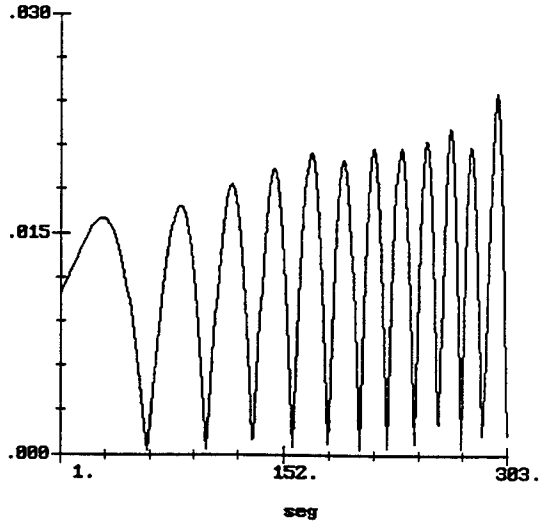

FIGURE A-22. 50-Ohm Load 0.9 GHz.

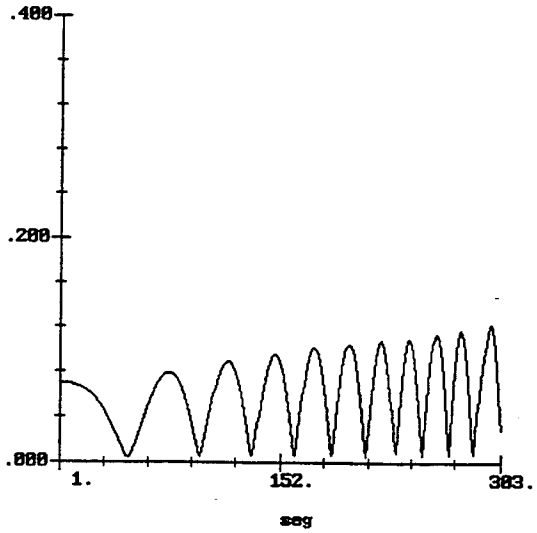

FIGURE A-23. 50-Ohm Load 0.8 GHz.

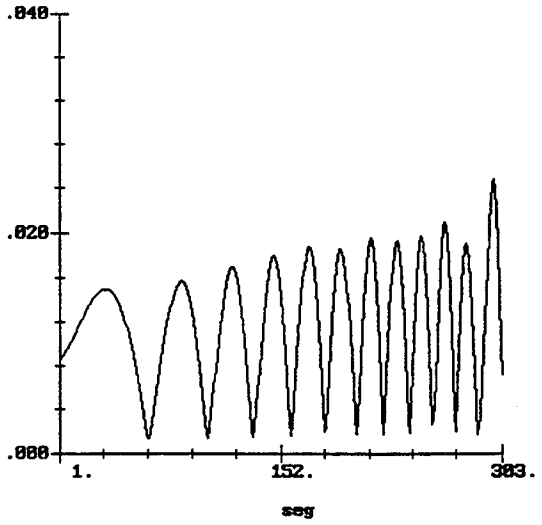

FIGURE A-24. 50-Ohm Load 0.7 GHz.

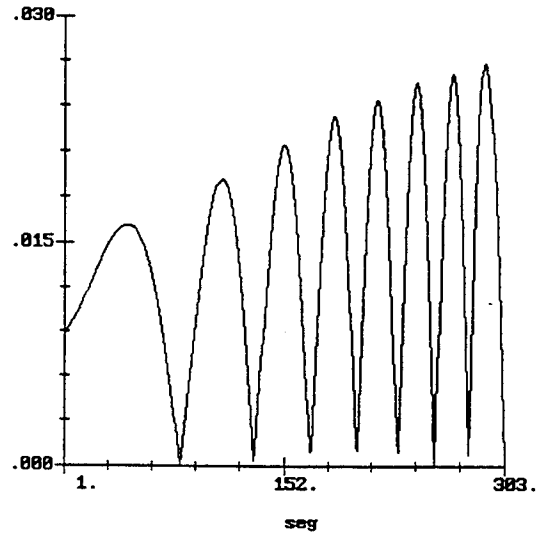

FIGURE A-25. 50-Ohm Load 0.6 GHz.

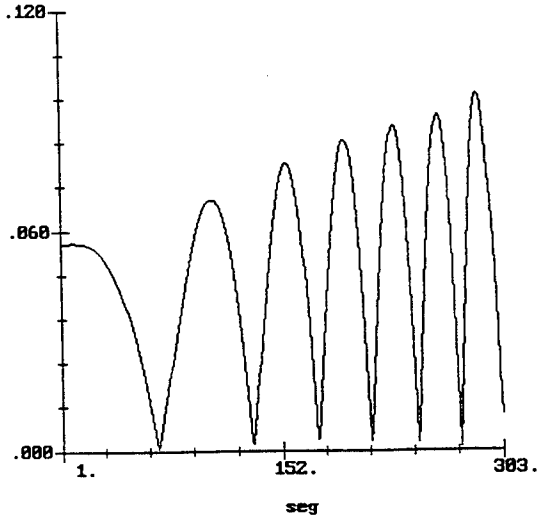

FIGURE A-26. 50-Ohm Load 0.5 GHz.

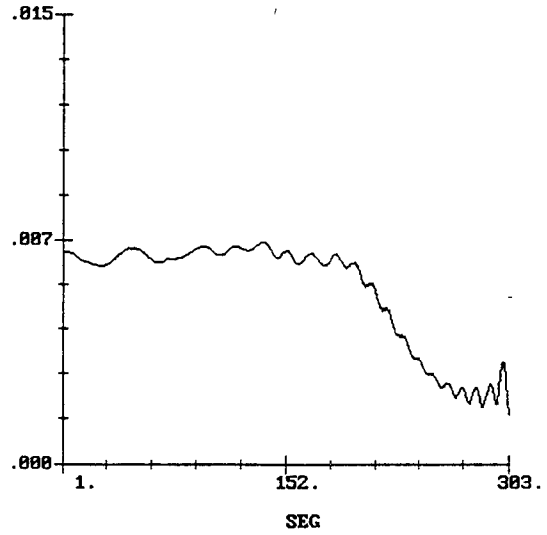

FIGURE A-27. 150-Ohm Load 1.4 GHz.

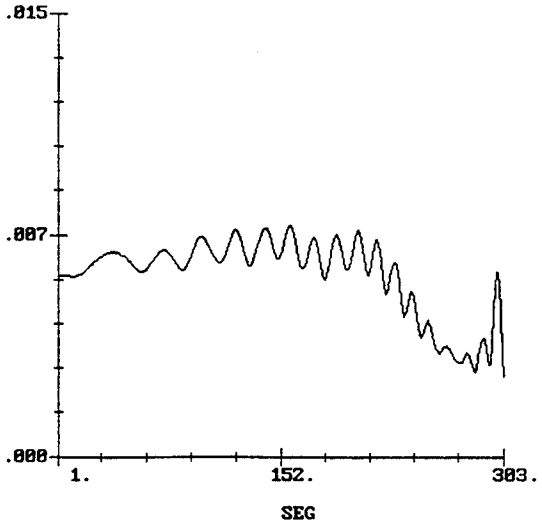

FIGURE A-28. 150-Ohm Load 1.3 GHz.

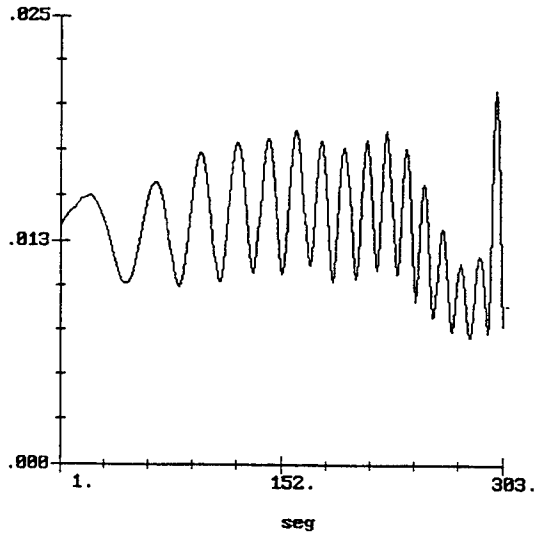

FIGURE A-29. 150-Ohm Load 1.2 GHz.

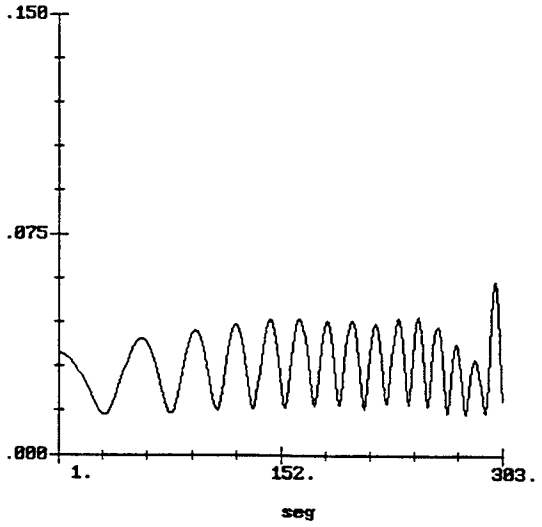

FIGURE A-30. 150-Ohm Load 1.1 GHz.

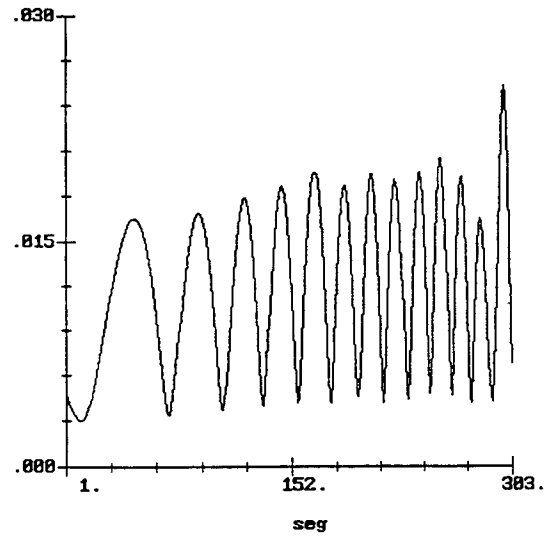

FIGURE A-31. 150-Ohm Load 1.0 GHz.

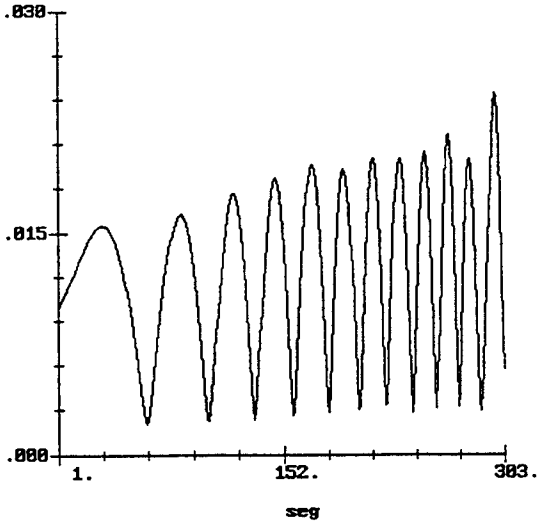

FIGURE A-32. 150-Ohm Load 0.9 GHz.

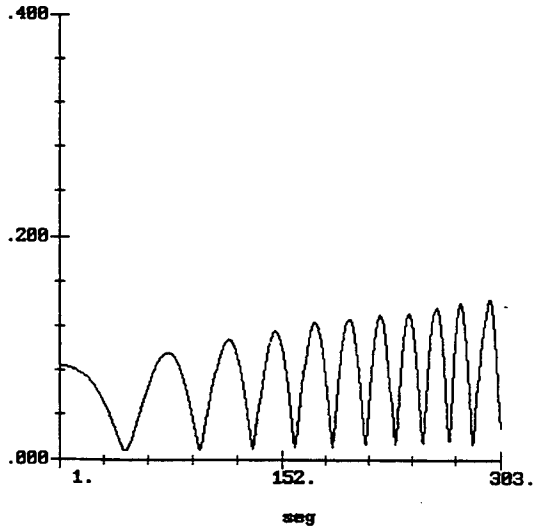

FIGURE A-33. 150-Ohm Load 0.8 GHz.

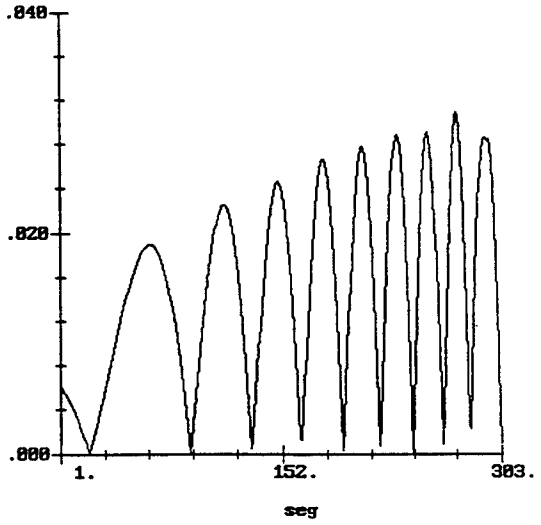

FIGURE A-34. 150-Ohm Load 0.7 GHz.

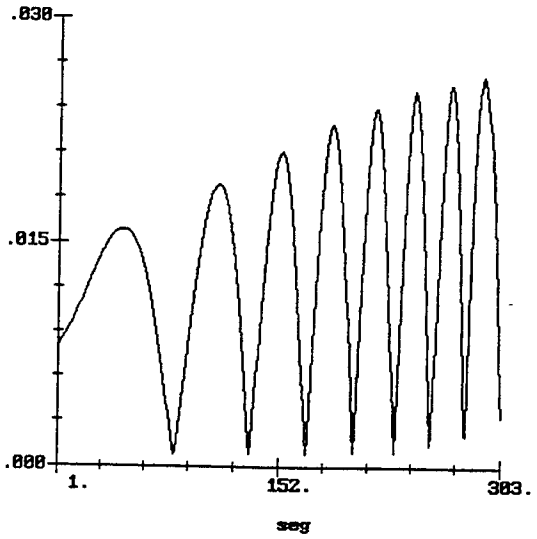

FIGURE A-35. 150-Ohm Load 0.6 GHz.

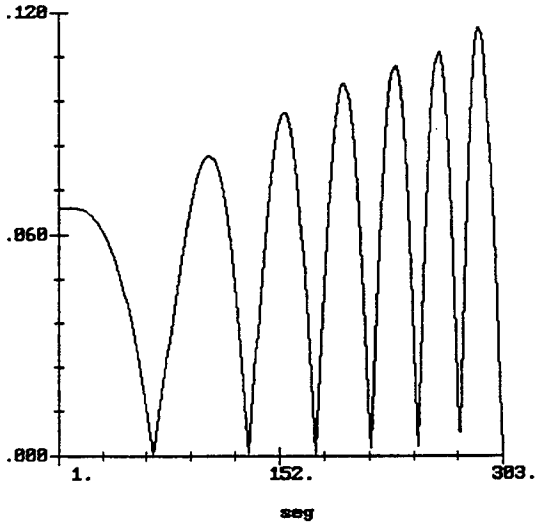

FIGURE A-36. 150-Ohm Load 0.5 GHz.

TABLE A-1. Spiral GEMACS Model, Center Fed Input Impedances.

Frequency (MHz)	Zin (open arms)	Zin 50-ohm loads)	Zin (150-ohm loads)
1600	67.3 + j35.1	65.5 + j34.7	65.9 + j35.6
1500	66 + j23.2	59.6 + j27.5	
1300	77.7 + j10.6	58.1 + j19.8	
1400	119 + j39.3	70.4 + j58.4	
1200	295 + j63.9	94.3 + j59.7	58.1 + j47.5
1100	97.4 - j 9.6	23.8 + j16.6	28.6 - j1.2
1000	92.9 - j357.8	66.3 + j127.5	148 - j148.4
900	2.72 + j91.9	16.8 + j116.9	20.9 + j99.7
800	0.71 + j4.88	3.59 + j13.7	6.6 + j9.8
700	2.47 - j160	11 - j116.6	26 - j126.4
600	0.43 + j113.7	4.6 + j129.6	10 + j124.4
500	0.46 +j14.8	0.59 + j17.7	1.5 + j17.2

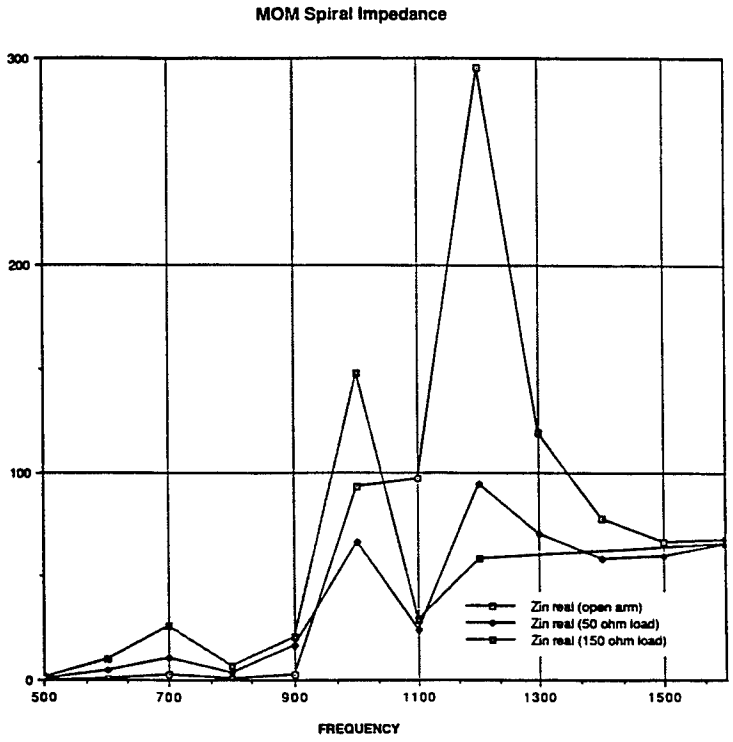

FIGURE A-37. Calculated Input Impedance For Open Circuit, 50- and 150-Ohm Loaded Antenna.

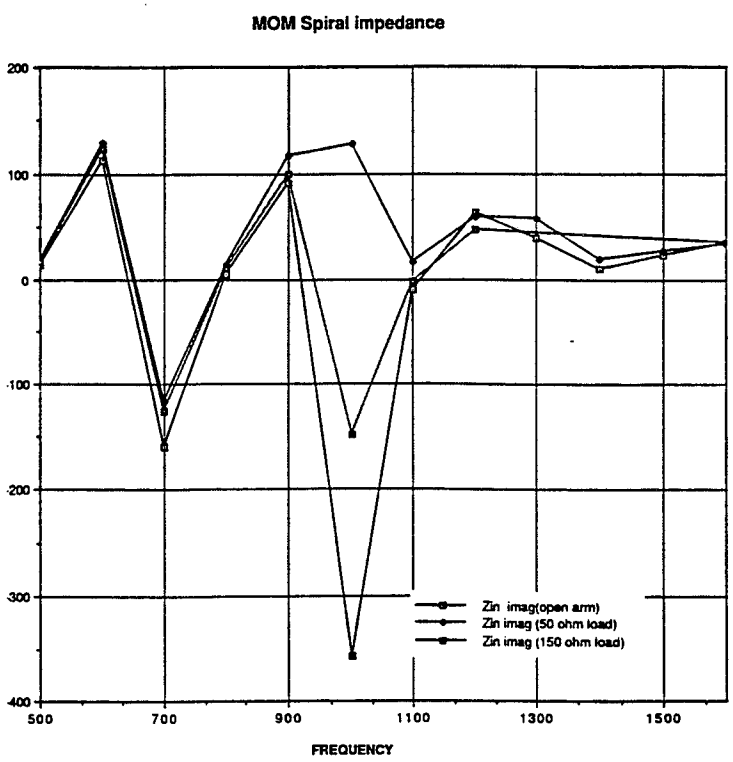

FIGURE A-38. Calculated Input Impedance For Open Circuit, 50- and 150-Ohm Loaded Antenna.

Appendix B.

GEMACS SPIRAL ANALYSIS ANALYTICALLY DETERMINED OPTIMUM ARM TERMINATION VALUES

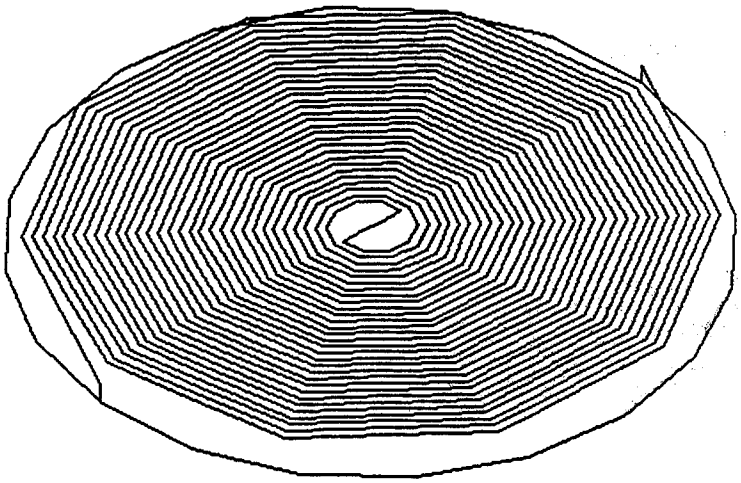

FIGURE B-1. Loaded Spiral Model.

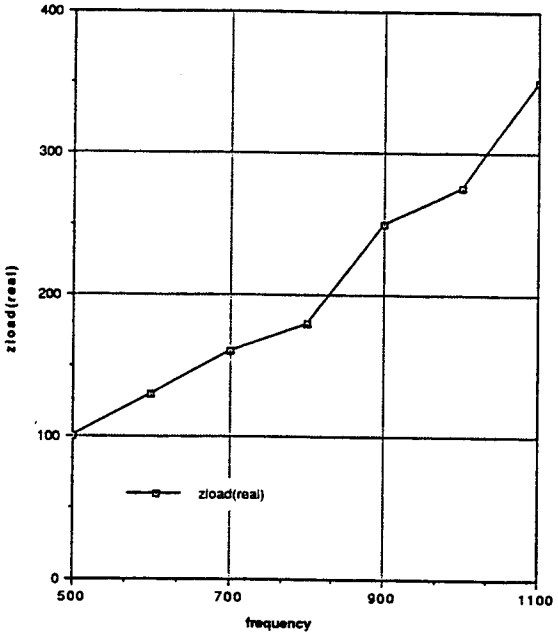

FIGURE B-2. Calculated "Best" Load Value For Spiral Model.

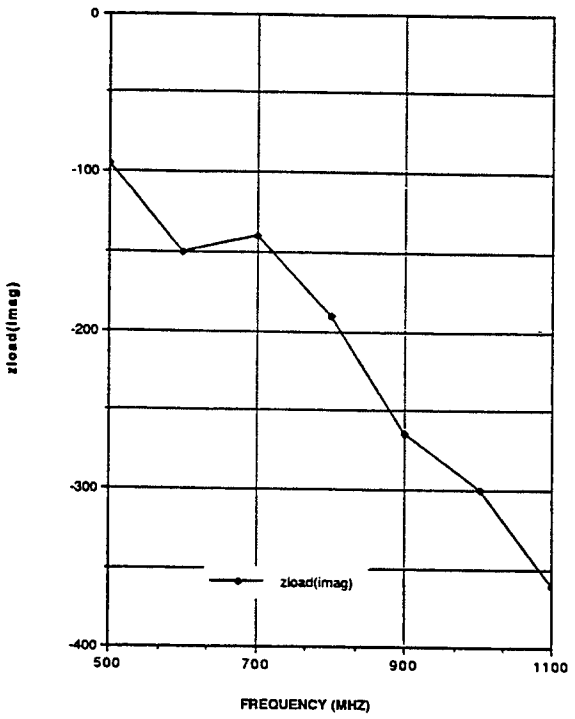

FIGURE B-3. Calculated "Best" Load Value For Spiral Model.

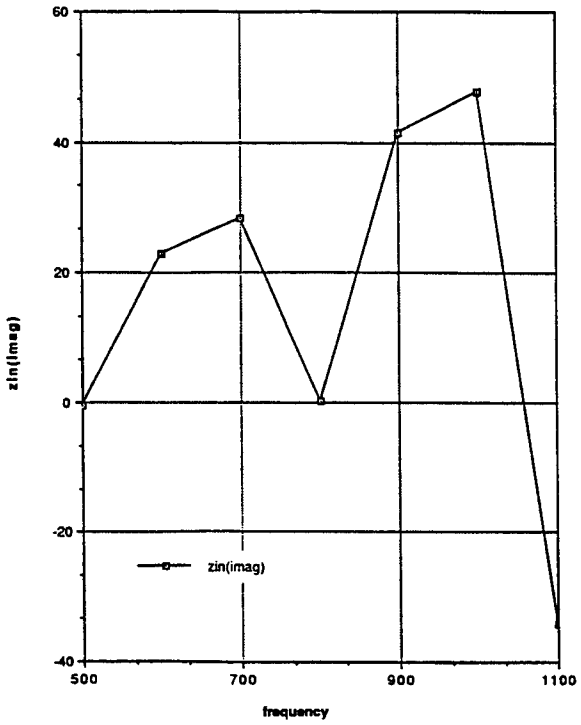

FIGURE B-4. Calculated Input Impedance Using Optimum Load.

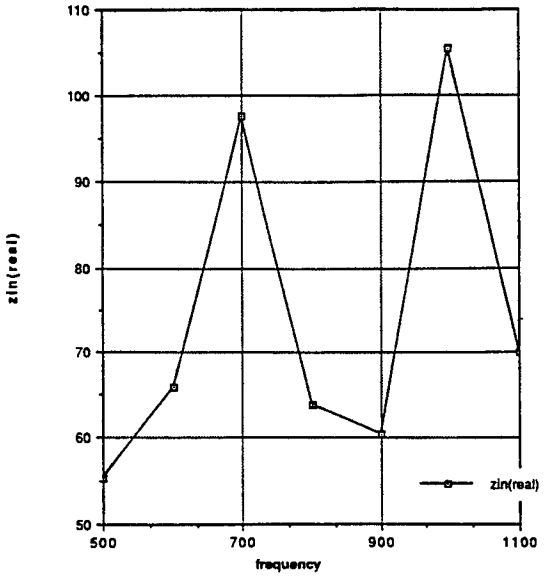

FIGURE B-5. Calculated Input Impedance Using Optimum Load.

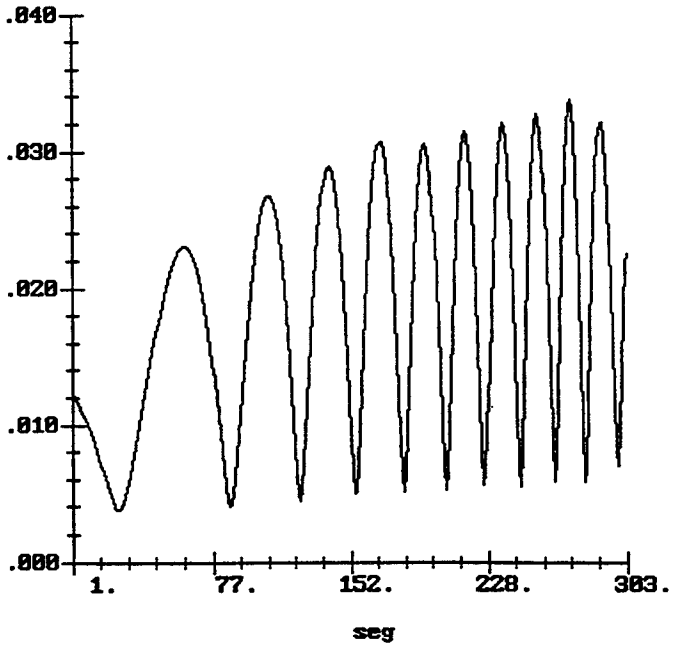

FIGURE B-6. 800-MHz Current Magnitude Versus Segment #. Arbitrary load z_{load} = 50 - j100, SWR 5.8.

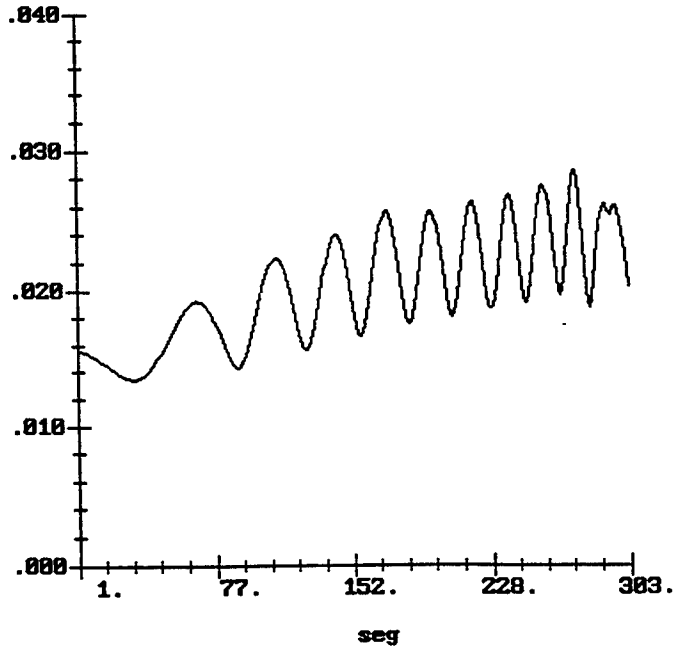

FIGURE B-7. 800-MHz Current Magnitude Versus Segment #. Optimum load z_{load} = 180 - j90, SWR 1.8.

INITIAL DISTRIBUTION

16 Naval Air Warfare Center Weapons Division, China Lake
- Code 472000D (C29)
- Code 472230D (C2953), D. Paolino (1)
- Code 472300D (C282), T. Hoppus (1)
- Code 472310D (C2824)
  - C. Hauser (1)
  - B. Joy (1)
  - D. Stapleton (1)
- Code 473000D (C27) (1)
- Code 474000D (C023) (1)
- Code 474160D (C02316)
  - D. Banks (1)
  - D. Bowling (1)
  - A. Martin (1)
- Code 474180D (C02318), P. Overfelt (1)
- Code 474700D (C0223) (4 (3 plus archives copy))

1 HQ 497 IG/INT, Falls Church (OUWG Chairman)
2 Defense Technical Information Center, Alexandria
3 AEL Defense Corporation, Lansdale, PA
- F. Euchler (1)
- D. Martin (1)
- J. Schuchardt (1)

1 Center for Naval Analyses, Alexandria, VA (Technical Library)
1 Comarco, Incorporated, Ridgecrest, CA (D. White)
1 Joseph Mosko, Boulder Creek, CA
1 University of Houston, Houston, TX (Department of Electrical and Computer Engineering, Dr. J. Williams)